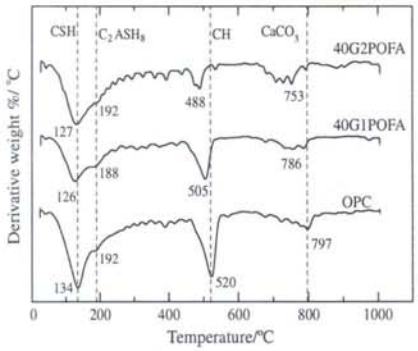

(a) Curing time 28 days

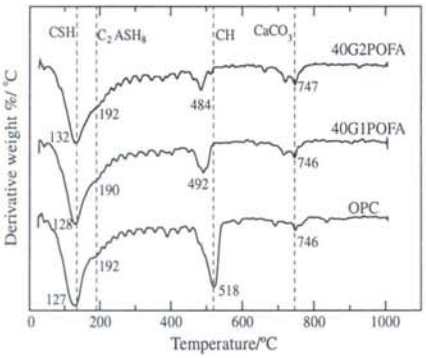

(b) Curing time 90 days

Fig. 7. DTG curve results of OPC paste and 40POFA pastes.

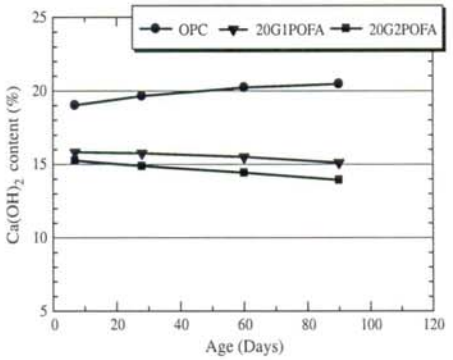

(a) Replacement 20 %

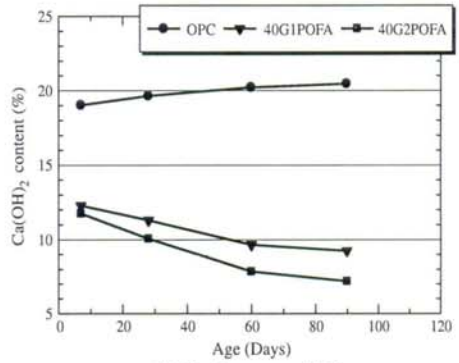

(b) Replacement 40 %

Fig. 8. $Ca(OH)_2$ content.

react with $Ca(OH)_2$ by the pozzolanic reaction. With a replacement ratio of 40% POFA, the $Ca(OH)_2$ contents of the 40G1POFA and 40G2POFA pastes were between 9.24–12.18% and 7.19–11.75% or reduced by approximately 24% and 39% as compared to the 40G1POFA and 40G2POFA pastes at 7 days, respectively. Moreover, the reduction of the $Ca(OH)_2$ contents of high replacement decreased more quickly than that of low replacement. These results suggest that the higher fineness palm oil fuel ash, which has a higher surface area, produces a greater pozzolanic reaction. In addition, the $Ca(OH)_2$ contents of pastes containing POFA decrease with increasing POFA content. These results agree with [9].

3.4. Pore size distribution of the cement paste

3.4.1. Total porosity of the cement paste

The results for the total porosity of all pastes at different ages are presented in Table 5. The total porosities of the OPC paste at 7, 28, 60 and 90 days were 22.8%, 20.1%, 17.4% and 16.6%, respectively, while the total porosities of the 20G1POFA and 40G1POFA pastes were 26.3%, 21.7%, 18.4%, 17.4% and 30.2%, 27.5%, 19.3%, 18.5% at 7, 28, 60 and 90 days, respectively, which were higher than that of the OPC paste. The results indicate that the total porosity of the pastes containing POFA with particle sizes that were the same as the cement was higher than that of the OPC cement paste. For the paste containing G2POFA at 7 days, the total porosity of the paste containing 20% palm oil fuel ash was lower than that of the OPC paste at all ages. In addition, the total porosity of the 40G2POFA paste at 60 days was 17.3%, which is slightly less than 17.4%, because the high fineness palm oil fuel ash had a faster pozzolanic reaction. The small particles showed a good filler effect in reducing the voids of the cement paste [32]. These results suggest that the addition of fine particles of palm oil fuel ash makes the blended cement paste denser [9].

Table 5
Total porosity of OPC paste and pastes containing ground palm oil fuel ash.

Mix no.	Symbol	Total porosity (%)			
		7 days	28 days	60 days	90 days
1	OPC	22.8	20.1	17.4	16.6
2	20G1POFA	26.3	21.7	18.4	17.4
3	40G1POFA	30.2	27.5	19.3	18.5
4	20G2POFA	20.5	17.0	15.5	11.4
5	40G2POFA	23.8	19.7	17.3	15.6

3.4.2. Effect of palm oil fuel ash fineness on the pore size distribution of the pastes

The cumulative pore volumes of pastes containing 20% and 40% POFA are shown in Figs. 9 and 10, respectively. As shown in Fig. 9, at 28 and 90 days, the cumulative pore volume of the 20G2POFA paste is the lowest. The high fineness of G2POFA had a fast pozzolanic reaction and a greater filler effect in the voids, thus reducing the porosity and increasing the density of the paste. For pastes containing 40% POFA, as shown in Fig. 10, the cumulative pore volumes of the 40G1POFA and 40G2POFA pastes at 28 days were higher than that of the OPC cement paste. However, at 90 days,

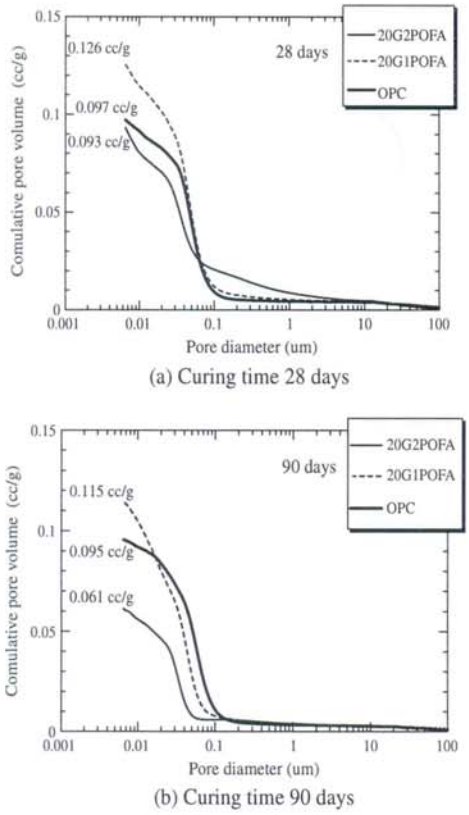

Fig. 9. Relationships between the cumulative pore volume and pore diameter of 20POFA paste.

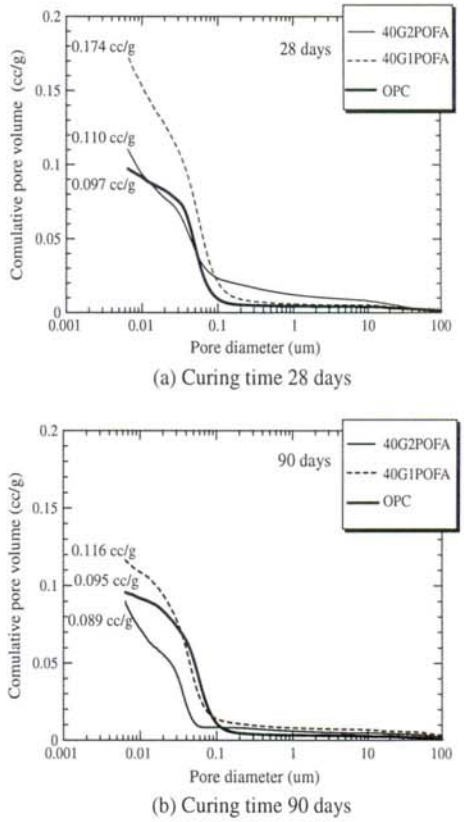

Fig. 10. Relationships between the cumulative pore volume and pore diameter of 40POFA paste.

the cumulative pore volume of the 40G2POFA paste was lower than that of the OPC paste due to the fact that the silicon dioxide (SiO_2) reacted with the calcium hydroxide $Ca(OH)_2$ and reduced the $Ca(OH)_2$ content by the pozzolanic reaction. Thus, the pore structure in the blended cement paste was refined; these results are in agreement with Li and Ding [38].

The critical pore size is defined as the inflection point on the cumulative pore volume and pore diameter plot or as the maximum of dv/d(log *D*). The critical pore size is the most frequent continuous pores [15,39]. For pastes containing 20% POFA at 28 days, as shown in Fig. 11, the critical pores sizes of the 20G1POFA and 20G2POFA pastes were 45.9 nm and 38.0 nm, respectively, which were distributed as medium capillary pores. These values were lower than that of the OPC paste (56.1 nm), which was specified to contain large capillary pores. At 90 days, the critical pore sizes of the OPC, 20G1POFA and 20G2POFA pastes were 54.6 nm, 41.7 nm and 31.0 nm, respectively, due to the reaction of the palm oil fuel ash with $Ca(OH)_2$. Consequently, the pore structure was transformed from coarser pores to finer pores [38]. These results suggest that the paste containing POFA had a lower critical pore size than the OPC cement paste.

For pastes at 40% POFA, the relationships between the differential pore volume and pore diameter at 28 and 90 days are shown in Fig. 12. The critical pore sizes of the 40G1POFA and 40G2POFA pastes at 28 and 90 days were 42.1 nm, 41.8 nm and 36.8 nm, 35.0 nm, respectively, which correspond to medium capillary pores. These values are smaller than that of the OPC cement paste. These results indicate that the paste with POFA contained critical pore sizes smaller than the OPC paste.

The results suggest that the total porosity of the paste containing POFA with the same particle size as cement was higher than that of the OPC cement paste, but the paste containing high fineness POFA had a lower total porosity than the OPC paste. In addition, the total porosity increased with an increase in the POFA replacement. Furthermore, the critical pore size of the paste with POFA was smaller than that of the OPC cement paste due to the filler effect, pozzolanic reaction, dispersion effect and precipitation effect [14,40]. The pore size structure of the pastes changed from coarser pores to finer pores [41]. Moreover, some researchers [42] have reported that the critical pore radius is the most important factor for permeability, and Halamickova et al. [15] found that the critical pore size affects water permeability and chloride ion diffusion.

3.4.3. Effect of palm oil fuel ash fineness on the average pore diameter of the cement paste

The results for the average pore diameter of all pastes are shown in Fig. 13. The average pore diameters of OPC paste at 7, 28, 60 and 90 days were 53.4 nm, 45.3 nm, 30.1 nm and 28.1 nm, respectively. For pastes containing G1POFA, which has the same particle sizes as OPC, the average pore diameters of the 20G1POFA and 40G1POFA pastes were lower than that of the OPC paste at all ages, while the total porosity was higher than that of the OPC paste. For pastes containing high fineness POFA, the average pore

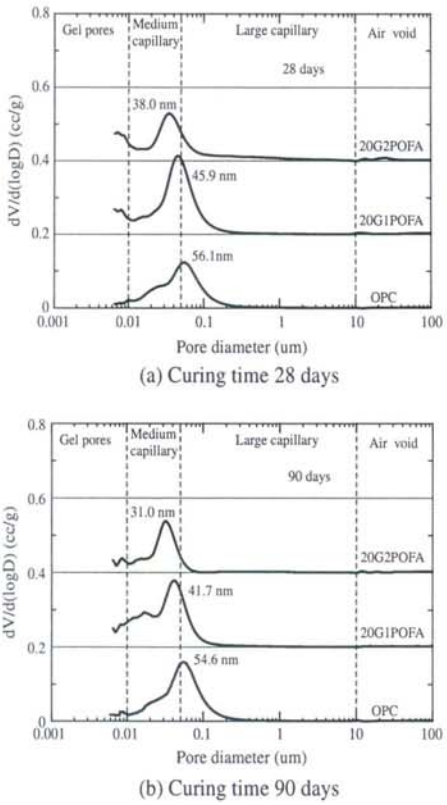

Fig. 11. Relationships between the differential pore volume and pore diameter of 20POFA paste.

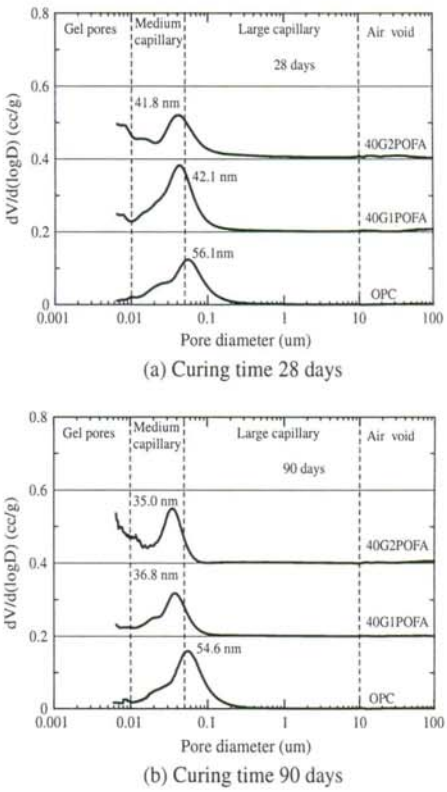

Fig. 12. Relationships between the differential pore volume and pore diameter of 40POFA paste.

diameters of the 20G2POFA and 40G2POFA pastes were lower than that of the OPC paste, and the total porosity of the 20G2POFA paste was lower than that of the OPC paste at all ages due to pore refinement and the reduction of calcium hydroxide in the paste [41,43]. These results indicate that the average pore diameter decreases with the use of POFA and with an increase in the replacement level, which again confirms that POFA with high fineness is more effective in reducing the average pore diameter as a result of the better dispersion, packing and pozzolanic reaction of the finer POFA particles. Similar results have been reported by other researchers [14,44].

3.5. Relationships between the compressive strength and total porosity of the pastes

Relationships between the compressive strength and total porosity of the pastes are shown in Fig. 14. The figures are divided into four regions. Region I shows pastes that have both a compressive strength and total porosity higher than those of the OPC paste. Region II presents the pastes of lower compressive strength but higher total porosity in comparison to the OPC paste. Region III contains pastes that have both lower compressive strength and lower total porosity than the OPC paste. Pastes in region VI are the best pastes, which have a lower total porosity and a higher compressive strength than the OPC paste. At 28 days, the 20G1POFA, 40G1POFA and 40G2POFA pastes were located in region III, while the 20G2POFA paste was located in region VI and was designated as the best paste because its

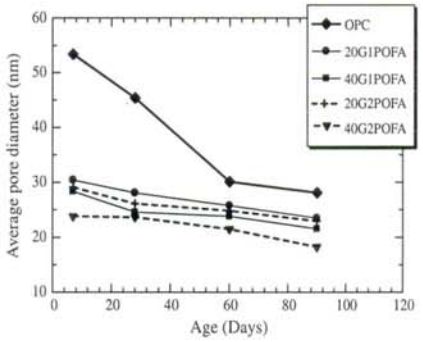

Fig. 13. Average pore diameter of curing days.

higher fineness ash can lead to greater filler effects, thus reducing the total porosity. Thus, the pastes containing POFA with high fineness increased the pozzolanic reaction rate and refined the pore structure of the paste.

At 90 days, the pastes containing POFA with the same particle size as cement were located in regions I and II. The 20G2POFA paste had a total porosity lower than that of the OPC paste, and the compressive strength was higher than that of the OPC paste, making it the best paste. However, the 40G2POFA paste had both

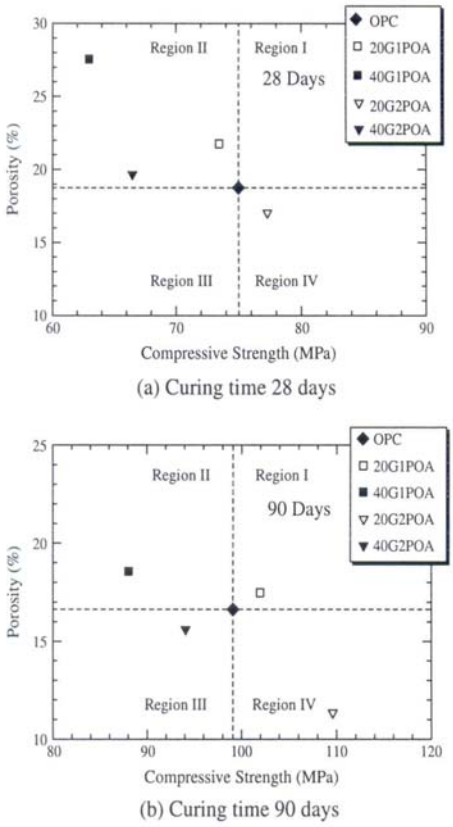

Fig. 14. Relationships between compressive strength and total porosity of paste.

a lower compressive strength and a lower total porosity than the OPC paste, which suggests that the high fineness POFA had a greater pozzolanic reaction and that the small particles of G2POFA more efficiently filled the voids of the paste. Therefore, the 20G2POFA paste was more homogeneous and had a lower total porosity than the OPC paste.

4. Conclusions

Based on the results of this study, the following conclusions can be drawn.

1. Fineness of palm oil fuel ash has the significant effect on the compressive strength of paste. Blended cement paste with high fineness palm oil fuel ash had a higher compressive strength than that with coarse palm oil fuel ash.
2. The paste containing palm oil fuel ash showed decreased $Ca(OH)_2$ contents with increases in the replacement and fineness of the ash. Moreover, the reduction of $Ca(OH)_2$ affected the increased peak intensity of the C–S–H and C_2ASH_8 phases with increasing curing time.
3. The reduction of the $Ca(OH)_2$ content in the POFA paste was due to the pozzolanic reaction and caused the pore size structure of the paste to change from coarser pores to finer pores. Thus, the critical pore size and average pore diameter of the paste containing palm oil fuel ash were lower than those of the OPC paste.
4. The amorphous content of palm oil fuel ash was approximately 67–70%. The use of palm oil fuel ash with high fineness to replace type I Portland cement at a rate of 20% resulted in good compressive strength. In addition, the total porosity of the paste was lower than that of OPC paste.

Acknowledgments

The authors would like to acknowledge the financial support of the Commission on Higher Education of Thailand for a grant under the Strategic Scholarships for Frontier Research Network for the Joint Ph.D. Program, Thai Doctoral degree. Thanks are also extended to the Thailand Research Fund (TRF) for financial support under the TRF Senior Research Scholar, Grant No. RTA5380002 and the TRF New Researcher Scholar, Grant No. MRG5280178.

References

[1] Hendrik G, Oss V, Padovani AC. Cement manufacture and the environment part ii: environmental challenges and opportunities. J Ind Ecol 2003;7:93–126.
[2] Chindaprasirt P, Rukzon S, Sirivivatnanon V. Resistance to chloride penetration of blended Portland cement mortar containing palm oil fuel ash, rice husk ash and fly ash. Constr Build Mater 2008;22(5):932–8.
[3] Chusilp N, Jaturapitakkul C, Kiattikomol K. Effects of LOI of ground bagasse ash on the compressive strength and sulfate resistance of mortars. Constr Build Mater 2009;23(12):3523–31.
[4] Tangchirapat W, Saeting T, Jaturapitakkul C, Kiattikomol K, Siripanichgorn A. Use of waste ash from palm oil industry in concrete. Waste Manage 2007;27(1):81–8.
[5] Chindaprasirt P, Homwuttiwong S, Jaturapitakkul C. Strength and water permeability of concrete containing palm oil fuel ash and rice husk-bark ash. Constr Build Mater 2007;21(7):1492–9.
[6] Chindaprasirt P, Rukzon S, Sirivivatnanon V. Effect of carbon dioxide on chloride penetration and chloride ion diffusion coefficient of blended Portland cement mortar. Constr Build Mater 2008;22(8):1701–7.
[7] Sata V, Jaturapitakkul C, Kiattikomol K. Utilization of palm oil fuel ash in high-strength concrete. J Mater Civ Eng 2004;16(6):623–8.
[8] Tangchirapat W, Jaturapitakkul C, Kiattikomol K. Compressive strength and expansion of blended cement mortar containing palm oil fuel ash. J Mater Civ Eng 2009;21(8):426–31.
[9] Chindaprasirt P, Jaturapitakkul C, Sinsiri T. Effect of fly ash fineness on microstructure of blended cement paste. Constr Build Mater 2007;21(7):1534–41.
[10] Barbhuiya SA, Gbagbo JK, Russell MI, Basheer PAM. Properties of fly ash concrete modified with hydrated lime and silica fume. Constr Build Mater 2009;23(10):3233–9.
[11] Chaipanich A, Nochaiya T. Thermal analysis and microstructure of Portland cement–fly ash–silica fume pastes. J Therm Anal Calorim 2010;99(2):487–93.
[12] Mindress S, Young JF. Concrete. Engle Cliffs: Prentice-Hall; 1981.
[13] Khatib JM, Wild S. Pore size distribution of metakaolin paste. Cem Concr Res 1996;26(10):1545–53.
[14] Chindaprasirt P, Jaturapitakkul C, Sinsiri T. Effect of fly ash fineness on compressive strength and pore size of blended cement paste. Cem Concr Compos 2005;27(4):425–8.
[15] Halamickova P, Detwiler RJ, Bentz DP, Garboczi EJ. Water permeability and chloride ion diffusion in Portland cement mortars: relationship to sand content and critical pore diameter. Cem Concr Res 1995;25(4):790–802.
[16] Chandara C, Sakai E, Azizli KAM, Ahmad ZA, Hashim SFS. The effect of unburned carbon in palm oil fuel ash on fluidity of cement pastes containing superplasticizer. Constr Build Mater 2010;24(9):1590–3.
[17] Jaturapitakkul C, Kiattikomol K, Tangchirapat W, Saeting T. Evaluation of the sulfate resistance of concrete containing palm oil fuel ash. Constr Build Mater 2007;21(7):1399–405.
[18] Kumar S, Kumar R. Mechanical activation of fly ash: effect on reaction, structure and properties of resulting geopolymer. Ceramics International 2011;37(2):533–41.
[19] Kumar S, Kumar R, Bandopadhyay A, Alex T, Ravi Kumar B, Das SK, et al. Mechanical activation of granulated blast furnace slag and its effect on the properties and structure of Portland slag cement. Cem Concr Compos 2008;30(8):679–85.
[20] Rukzon S, Chindaprasirt P, Mahachai R. Effect of grinding on chemical and physical properties of rice husk ash. Int J Miner Metall Mater 2009;16(2):242–7.
[21] Bouzoubaâ N, Zhang MH, Bilodeau A, Malhotra VM. The effect of grinding on the physical properties of fly ashes and a Portland cement clinker. Cem Concr Res 1997;27(12):1861–74.
[22] ASTM C109. Standard test method for compressive strength of hydraulic cement mortars (using 2-in. or [50 mm] cube specimens). Annual book of ASTM standards, vol. 04.01; 2001. p. 83–8.

[23] Bai J, Chaipanich A, Kinuthia JM, O'Farrell M, Sabir BB, Wild S, et al. Compressive strength and hydration of wastepaper sludge ash-ground granulated blastfurnace slag blended pastes. Cem Concr Res 2003;33(8):1189–202.
[24] El-Jazairi B, Illston JM. A simultaneous semi-isothermal method of thermogravimetry and derivative thermogravimetry, and its application to cement pastes. Cem Concr Res 1977;7(3):247–57.
[25] Chaipanich A, Nochaiya T. Thermal analysis and microstructure of Portland cement–fly ash–silica fume pastes. J Therm Anal Calorim 2010;99:487–93.
[26] Galle C. Effect of drying on cement-based materials pore structure as identified by mercury intrusion porosimetry: a comparative study between oven-, vacuum-, and freeze-drying. Cem Concr Res 2001;31(10):1467–77.
[27] Konecny L, Naqvi SJ. The effect of different drying techniques on the pore size distribution of blended cement mortars. Cem Concr Res 1993;23(5):1223–8.
[28] Washburm EW. Note on method of determining the distribution of pore size in porous materials. Proc Natl Acad Sci USA 1921;7:115–6.
[29] Awal ASMA, Hussin MW. The effectiveness of palm oil fuel ash in preventing expansion due to alkali–silica reaction. Cem Concr Compos 1997;19(4):367–72.
[30] ASTM C618. A standard specification for coal fly ash and raw or calcined natural pozzolan for use as a mineral admixture in concrete. Annual book of ASTM standards, vol. 04.02; 2001. p. 310–3.
[31] Sata V, Jaturapitakkul C, Rattanashotinunt C. Compressive strength and heat evolution of concretes containing palm oil fuel ash. J Mater Civ Eng 2010;22.
[32] Isaia GC, Gastaldini ALG, Moraes R. Physical and pozzolanic action of mineral additions on the mechanical strength of high-performance concrete. Cem Concr Compos 2003;25(1):69–76.
[33] Mehta PK, Aietcin P-CC. Principles underlying production of high-performance concrete. Cem Concr Aggr 1990;12(2):70–8.
[34] Gopalan MK. Nucleation and pozzolanic factors in strength development of class F fly ash concrete. ACI Mater J 1993;90(2):117–21.
[35] Montgomery DG, Hughes DC, Williams RIT. Fly ash in concrete – a microstructure study. Cem Concr Res 1981;11(4):591–603.
[36] Nochaiya T, Wongkeo W, Pimraksa K, Chaipanich A. Microstructural, physical, and thermal analyses of Portland cement–fly ash–calcium hydroxide blended pastes. J Therm Anal Calorim 2010;100(1):101–8.
[37] Vedalakshmi R, Sundara Raj A, Srinivasan S, Ganesh Babu K. Quantification of hydrated cement products of blended cements in low and medium strength concrete using TG and DTA technique. Thermochim Acta 2003;407(1–2):49–60.
[38] Li Z, Ding Z. Property improvement of Portland cement by incorporating with metakaolin and slag. Cem Concr Res 2003;33(4):579–84.
[39] Pipilikaki P, Beazi-Katsioti M. The assessment of porosity and pore size distribution of limestone Portland cement pastes. Constr Build Mater 2009;23(5):1966–70.
[40] Poon CS, Wong YL, Lam L. The influence of different curing conditions on the pore structure and related properties of fly-ash cement pastes and mortars. Constr Build Mater 1997;11(7-8):383–93.
[41] Poon CS, Lam L, Kou SC, Wong YL, Wong R. Rate of pozzolanic reaction of metakaolin in high-performance cement pastes. Cem Concr Res 2001;31(9):1301–6.
[42] Ye G, Lura P, van Breugel K. Modelling of water permeability in cementitious materials. Mater Struct 2006;39(9):877–85.
[43] Chindaprasirt P, Rukzon S. Strength, porosity and corrosion resistance of ternary blend Portland cement, rice husk ash and fly ash mortar. Constr Build Mater 2008;22(8):1601–6.
[44] Frías M, Cabrera J. Pore size distribution and degree of hydration of metakaolin–cement pastes. Cem Concr Res 2000;30(4):561–9.

2. Napia, C. , Sinsiri, T.*, Jaturapitakkul C., Chindaprasirt, P., 2012, Leaching of heavy metals from solidified waste using Portland cement and zeolite as a binder, Waste Management, 32 (2012), 1459-1467. (IF= 2.353)

Waste Management 32 (2012) 1459–1467

Contents lists available at SciVerse ScienceDirect

Waste Management

journal homepage: www.elsevier.com/locate/wasman

Leaching of heavy metals from solidified waste using Portland cement and zeolite as a binder

Chuwit Napia [a], Theerawat Sinsiri [a,*], Chai Jaturapitakkul [b], Prinya Chindaprasirt [c]

[a] School of Civil Engineering, Institute of Engineering, Suranaree University of Technology, Nakorn Ratchasima 30000, Thailand
[b] Department of Civil Engineering, Faculty of Engineering, King Mongkut's University of Technology Thonburi, Bangkok 10140, Thailand
[c] Sustainable Infrastructure Research and Development Center, Department of Civil Engineering, Faculty of Engineering, Khon Kaen University, Khon Kaen 40002, Thailand

ARTICLE INFO

Article history:
Received 1 July 2011
Accepted 27 February 2012
Available online 31 March 2012

Keywords:
Leaching
Heavy metal
Solidified waste
Zeolite

ABSTRACT

This study investigated the properties of solidified waste using ordinary Portland cement (OPC) containing synthesized zeolite (SZ) and natural zeolite (NZ) as a binder. Natural and synthesized zeolites were used to partially replace the OPC at rates of 0%, 20%, and 40% by weight of the binder. Plating sludge was used as contaminated waste to replace the binder at rates of 40%, 50% and 60% by weight. A water to binder (w/b) ratio of 0.40 was used for all of the mixtures. The setting time and compressive strength of the solidified waste were investigated, while the leachability of the heavy metals was determined by TCLP. Additionally, XRD, XRF, and SEM were performed to investigate the fracture surface, while the pore size distribution was analyzed with MIP.

The results indicated that the setting time of the binders marginally increased as the amount of SZ and NZ increased in the mix. The compressive strengths of the pastes containing 20 and 40 wt.% of NZ were higher than those containing SZ. The compressive strengths at 28 days of the SZ solidified waste mixes were 1.2–31.1 MPa and those of NZ solidified waste mixes were 26.0–62.4 MPa as compared to 72.9 MPa of the control mix at the same age. The quality of the solidified waste containing zeolites was better than that with OPC alone in terms of the effectiveness in reducing the leachability. The concentrations of heavy metals in the leachates were within the limits specified by the US EPA. SEM and MIP revealed that the replacement of Portland cement by zeolites increased the total porosity but decreased the average pore size and resulted in the better containment of heavy ions from the solidified waste.

1. Introduction

Currently, over 80% of the hazardous wastes are from industrial processes. The sludge, heavy metals, oils and infectious waste are the most abundant hazardous wastes. The amount of industrial waste and hazardous waste from industrial plants increases every year. The toxic wastes containing heavy metals are, therefore, causing serious environmental problems in the contamination of water, air and soil. It is an issue that deserves attention to find ways to properly and appropriately capture the waste.

The hazardous waste water from industries is released from industrial facilities and is also causing critical environmental problems. The treatment processes could reduce the concentrations of the toxic waste depending on the condition of the sediment's dry residue. However, the final disposal of the waste sediment is still not safe in terms of storage and transportation because some heavy metals remain unstable and may leak into the environment. To solve the problem, the method of reducing or storing hazardous toxic waste is required to stop the leaching of toxic substances to the environment.

Solidification is a process used to treat hazardous waste from industrial plants, particularly hazardous substances or inorganic substances contaminated by heavy metals. The hazardous substances are stored in the structure by chemical bonding which neutralizes them and reduces the chance of spreading. The placeholder used in this process is normally Portland cement blended with pozzolanic materials such as fly ash, rice husk ash and silica fume. Solidification eases the safe transport of the solid cast mass and allows disposal in a landfill.

Zeolites are framework silicates consisting of interlocking tetrahedrons of SiO_4 and AlO_4. The alumino-silicate structure is negatively charged and attracts the positive ions that reside within the zeolites. This results in large vacant spaces or cages in their structures that allow space for large cations such as sodium, potassium, barium, calcium and even relatively large molecules as well as cation groups of water, ammonia, carbonate ions and nitrate ions (Feng et al., 2000). The spaces are interconnected and form long and wide channels of various sizes depending on the minerals. These channels allow easy movement of the resident ions and molecules into and

* Corresponding author. Tel.: +66 4422 4420; fax: +66 4422 4607.
E-mail address: sinsiri@sut.ac.th (T. Sinsiri).

0956-053X/$ - see front matter © 2012 Elsevier Ltd. All rights reserved.
http://dx.doi.org/10.1016/j.wasman.2012.02.011

Table 1
Sample mix proportions (by weight).

Binder			S (%)	w/b	Symbol
OPC (%)	SZ (%)	NZ (%)			
100	–	–	–	0.4	OPC100
			40	0.4	OPC40S
			50	0.4	OPC50S
			60	0.4	OPC60S
80	20	–	–	0.4	OPC20SZ
			40	0.4	OPC20SZ40S
			50	0.4	OPC20SZ50S
			60	0.4	OPC20SZ60S
60	40	–	–	0.4	OPC40SZ
			40	0.4	OPC40SZ40S
			50	0.4	OPC40SZ50S
			60	0.4	OPC40SZ60S
80	–	20	–	0.4	OPC20NZ
			40	0.4	OPC20NZ40S
			50	0.4	OPC20NZ50S
			60	0.4	OPC20NZ60S
60	–	40	–	0.4	OPC40NZ
			40	0.4	OPC40NZ40S
			50	0.4	OPC40NZ50S
			60	0.4	OPC40NZ60S

out of the structure. The zeolites are thus characterized by their ability to lose and absorb water without damaging their crystal structures (Quanlin and Naiqian, 2005).

Clinoptilolite is a naturally occurring zeolite that forms through the devitrification (the conversion of glassy material to crystalline material) of volcanic ash in lake and marine waters. It is the most studied of all zeolites and is widely regarded as the most useful. Clinoptilolite has a particularly high cation exchange capacity which provides many useful properties (Poon et al., 2000). Clinoptilolite is used in many applications such as chemical sieves, gas absorbers, feed additives, food additives, odor control agents and water filters for municipality, residential drinking water and aquariums (Feng and Peng, 2005). Clinoptilolite is well suited for these applications because of its large amount of pore space, high resistance to extreme temperatures and chemically neutral basic structure.

Sludge produced by the metal plating industry is generally considered to be "hazardous waste" because of its toxic heavy metal content. Solidification techniques applied prior to the deposition of this waste in landfills provide good results allowing the safe disposal of inorganic sludge. The use of materials such as zeolite with its pozzolanic property and the ability to bind metal ions generally gives a good performance. The solidification can store a large amount of sludge and help protecting the environment. This study, therefore, aims to investigate an effective solidification technique for sludge from a metal plating factory using both natural and synthesized zeolites in corporation with Portland cement.

2. Experimental investigation

2.1. Materials

The materials used were ordinary Portland cement (OPC) per ASTM C150, sodium aluminum silicate ($Na_{96}Al_{96}Si_{96}O_{384}$) as synthesized zeolite (SZ), clinoptilolite ($(Na,K,Ca)_6(Si{\cdot}Al)_{36}O_{72}20H_2O$) as natural zeolite (NZ), sludge (S) from the treatment of wastewater from a nickel plating plant and tap water. The S contained 35% water and 65% solid. It was dried and then sieved through a No. 100 sieve.

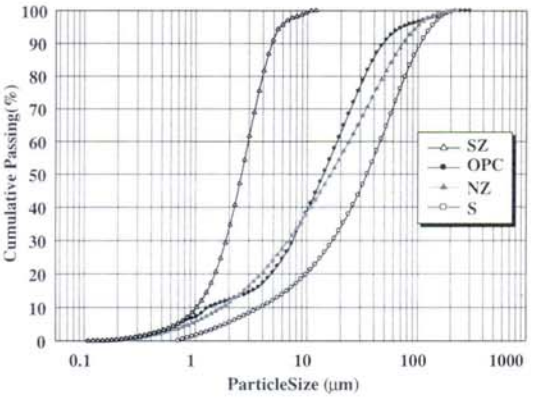

Fig. 1. Particle size distribution of OPC, SZ, NZ and S.

2.2. Mixture proportions

The sludge waste was solidified using OPC containing SZ and NZ as a binder. Zeolites were used to partially replace OPC at rates of 0%, 20%, and 40% by weight of the binder. The plating sludge was used to replace the binders at the rates of 40%, 50% and 60% by weight. A constant water to binder (w/b) ratio of 0.40 was used. The pastes were mixed in a mechanical mixer, and the specimens were cast in 50-mm cube molds. The fresh samples were covered with a plastic sheet to prevent water evaporation. After casting for 24 h, the samples were removed from the molds and cured in saturated lime water (Table 1).

3. Test programs

3.1. Specific gravity and particle size

The specific gravity of OPC, SZ, NZ and S was measured in accordance with ASTM C188, and their particle sizes were measured using laser particle size analysis.

3.2. Normal consistency

The normal consistency of the pastes was measured in accordance with ASTM C187 using Vicat apparatus.

3.3. Compressive strength

The compressive strength of the solidified waste was tested in accordance with ASTM C109 at ages of 7, 28, and 90 days. Five samples were tested for each age group.

Table 2
Specific gravity, median particle size and surface area of OPC, SZ, NZ and S.

Sample	Specific gravity	Mean particle size d_{50} (μm)	Surface area[a] (cm^2/g)
OPC	3.15	14.12	2600
SZ	1.87	2.51	32,500
NZ	2.09	16.17	5400
S	2.14	34.81	1900

[a] BET analysis.

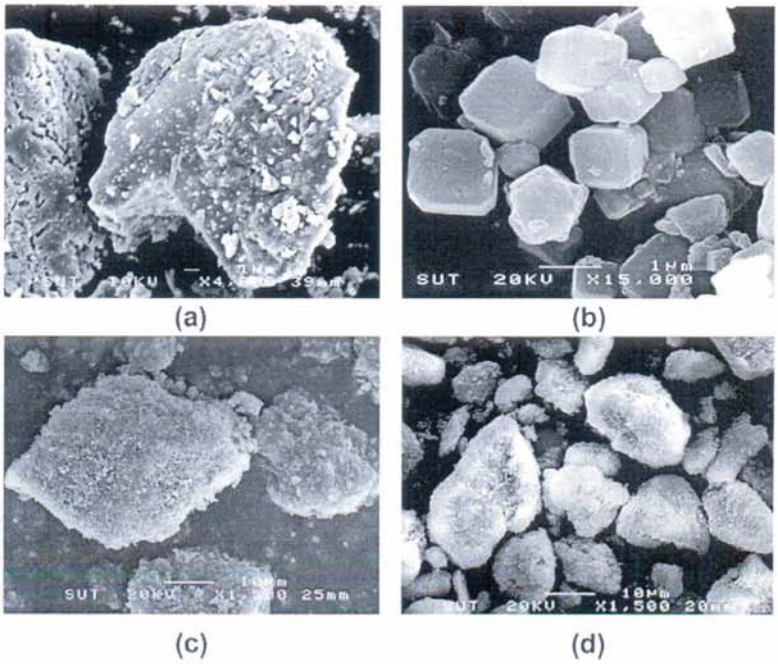

Fig. 2. SEM micrographs of (a) OPC at 4000 time, (b) SZ at 15,000 time, (c) NZ at 1500 time and (d) S at 1500 times.

Table 3
Chemical composition of materials.

Chemical composition (%)	OPC	SZ	NZ	S
SiO_2	19.85	65.3	75.32	5.53
Al_2O_3	4.49	26.18	10.28	3.78
Fe_2O_3	3.56	0.03	2.66	–
CaO	66.96	0.12	3.95	25.32
MgO	1.36	0.08	1.2	–
K_2O	0.34	2.64	4.29	–
Na_2O	–	1.87	0.89	–
NiO	–	–	–	40.88
CuO	–	–	–	13.08
ZnO	–	–	–	10.33
CrO	–	–	–	0.64
LOI	0.98	5.65	2.3	0.44

3.4. Scanning electron microscopy (SEM)

A JEOL scanning electron microscope (model JSM6400) was used to examine the phase development and microstructure of the solidified plating waste. The paste cubes at the ages of 7 and 28 days were broken and the fractions in the middle part of the specimens were used for the analyses. The solid was placed on a brass stub sample holder with double stick carbon tape. Then, the sample was dried using infrared light for 5 min. Subsequently, the sample was coated with a layer of gold approximately 20–25 Å thick using a blazer sputtering coater. Micrographs were recorded at 12 kV and 500–10,000× magnifications (Chindaprasirt et al., 2005).

3.5. X-ray diffractometer (XRD) and X-ray fluorescence (XRF) analyses

The XRD scans were performed for $2\theta^{\circ}$ between 10° and 70°, with an increment of 0.03°/step and a scan speed of 0.5 s/step. XRD analysis using Bruker's TOPAS software and using wavelength dispersive XRF (WDXRF). The positions of the diffraction peaks were identified by comparison to reference database compounds (Chindaprasirt et al., 2005).

3.6. Mercury intrusion porosimetry procedure (MIP)

The pore diameter distribution in the hardened cement pastes was measured by mercury intrusion porosimetry (MIP) at a pressure capacity of 228 MPa. After curing for 7, 28 and 90 days, the samples were split from the middle portion of the hardened blended cement paste. To stop the hydration reaction, the samples were submerged directly into liquid nitrogen for 5 min and were then evacuated at a pressure of 0.5 Pa at −40 °C for 48 h. This method has been used previously to stop the hydration reaction of cement paste (Chindaprasirt et al., 2007).

3.7. Toxicity characteristic leaching procedure (TCLP)

The metal leaching from the solidified plating waste cured for 7, 28 and 90 days and was assessed using the TCLP as defined by the US EPA (Li et al., 2001). The samples were crushed to reduce the particle size to less than 9.5 mm. The crushed sample was extracted using an acetic acid solution (pH 2.88) in a volume with a weight equal to 20 times the weight of the sample. The extraction vessels were rotated in an end-over-end manner at 30 rpm for 18 h. The leachate was filtered through a 0.45-μm membrane filter to remove suspended solids and was then divided into two portions. One portion was used for a pH measurement, and the other was used for the determination of the metals present in the leachate by ICP-AES. Each extraction was performed in triplicate, and the average value was reported to ensure the reproducibility of the data (Asavapisit et al., 2005).

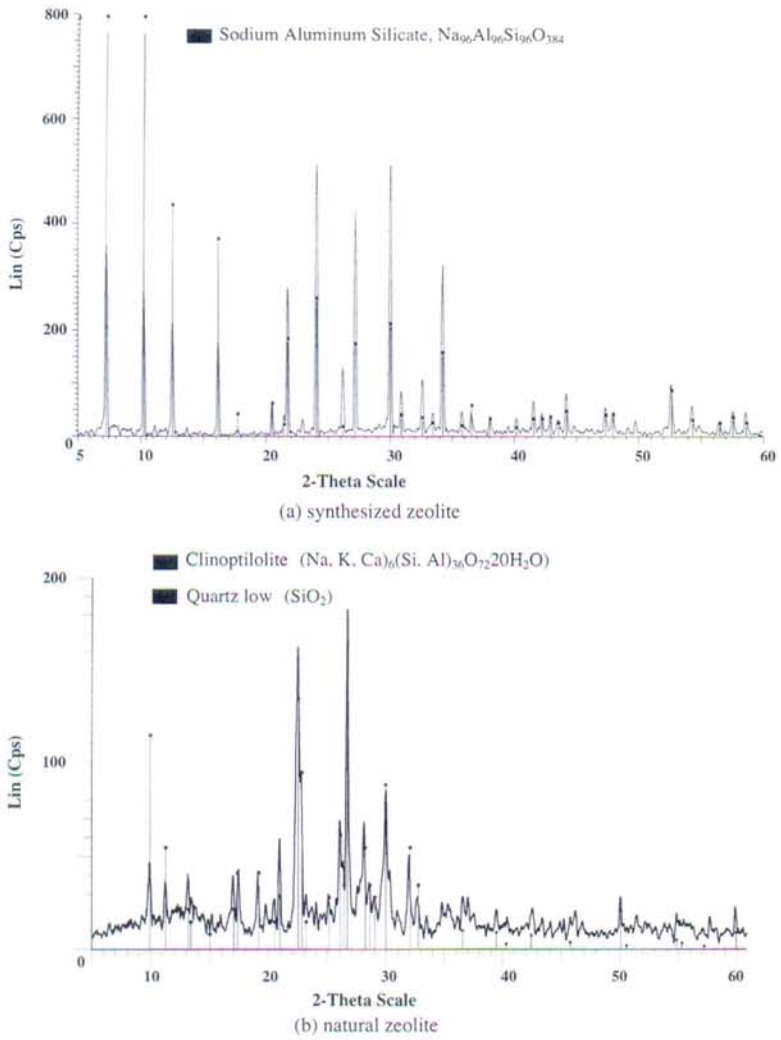

Fig. 3. XRD patterns of synthesized zeolite and natural zeolites.

4. Results and discussion

4.1. Properties of materials

4.1.1. Physical results for OPC, SZ, NZ and S

The specific gravity and median particle size (d_{50}) of the OPC, SZ, NZ and S are shown in Table 2. The median particle size (d_{50}) of the OPC was approximately 14.1 μm, while those of SZ, NZ and S were 2.5, 16.2 and 34.8 μm, respectively. The surface areas of the OPC, SZ, NZ and S were 2600, 32,500, 5400 and 1900 cm^2/g, respectively. The particle size distribution for the OPC, SZ, NZ and S was measured with a Mastersizer and is graphically shown in Fig. 1. For the OPC, NZ and S, the particle shape was solid and angular, whereas the surface of the SZ was smooth and exhibited a hexagonal character (Fig. 2).

4.1.2. Chemical composition and material patterns

Table 3 shows the chemical composition of the OPC, SZ, NZ and S, which was analyzed by XRF. SZ and NZ were found to be mainly SiO_2 and Al_2O_3. As can be seen, these two components were 90% for SZ and 85% for NZ. Additionally, the main elements of S were NiO (40.88%), CaO (25.32%), CuO (13.08%) and ZnO (10.33%).

Fig. 3 shows the XRD patterns for the SZ and NZ. The figure indicates that the intensity peak of sodium aluminum silicate ($Na_{96}Al_{96}Si_{96}O_{384}$) and $(Na,K,Ca)_6(Si{\cdot}Al)_{36}O_{72}20H_2O$ appeared at 0–60° (2θ).

4.2. Properties of pastes

4.2.1. Normal consistency of pastes

The normal consistency of OPC100 was found to be 25.5%. Higher replacement of SZ and NZ resulted in a higher normal consistency. For example, the normal consistencies of pastes OPC20SZ, OPC40SZ, OPC20NZ and OPC40NZ were 32.4%, 34.4%, 31.2% and 32.0%, respectively. The normal consistency of pastes containing SZ and NZ, which have a higher fine content, was higher than those containing coarser zeolites. This occurs because the particles of SZ and NZ have a higher fine content and a higher porosity; thus, they absorb more water, which results in greater water consumption.

Table 4
Setting time and compressive strength of the solidified wastes.

Sample	Time (min)		Compressive Strength (MPa)		
	Initial setting time	Final setting time	7-day	28-day	90-day
OPC100	132	181	53.8	72.9	79.4
OPC40S	148	192	0.9	1.3	1.5
OPC50S	151	195	0.6	1.0	1.2
OPC60S	154	197	0.5	0.8	1.1
OPC20SZ	141	185	21.6	31.1	38.2
OPC20SZ40S	149	186	2.1	13.5	16.1
OPC20SZ50S	152	186	1.3	4.9	10.7
OPC20SZ60S	156	185	0.8	1.4	2.0
OPC40SZ	143	187	10.2	23.4	26.9
OPC40SZ40S	149	188	0.3	6.0	17.4
OPC40SZ50S	151	189	0.3	4.2	13.6
OPC40SZ60S	152	190	0.1	1.2	3.2
OPC20NZ	133	183	52.0	62.4	71.1
OPC20NZ40S	135	184	43.4	57.3	65.2
OPC20NZ50S	135	185	35.7	49.1	58.4
OPC20NZ60S	136	186	30.5	41.3	50.3
OPC40NZ	134	184	40.5	50.7	61.3
OPC40NZ40S	135	184	19.5	36.2	43.4
OPC40NZ50S	136	185	15.2	31.5	39.3
OPC40NZ60S	136	187	12.1	26.0	33.8

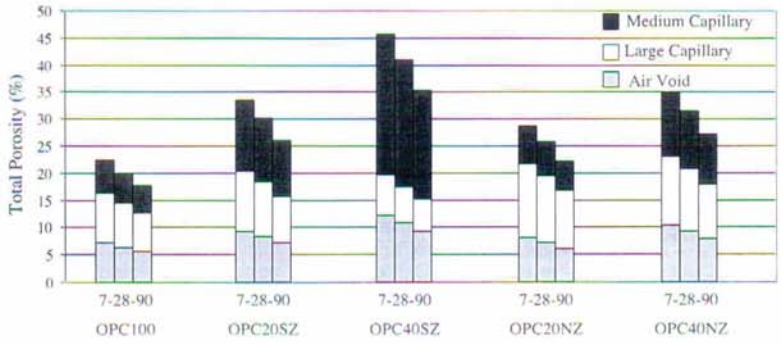

Fig. 4. Total porosity of cement paste and blended cement pastes at 7, 28 and 90 days.

4.2.2. Setting time of blended cement pastes and pastes containing solidified plating waste

The setting times of the blended cement pastes containing SZ and NZ were similar to those of the Portland cement paste. For example, the final setting times of OPC paste, was 181 min. The initial setting time of mixes with SZ was 185 and 187 min and those with NZ were 183 and 184 min. For the incorporation of S, the initial setting time was increased to 148–154 min and the final setting times to 191–192 min. The similar or slightly increase in the setting time were probably due to the pastes mixed with zeolites have higher water contents at normal consistency than Portland cement paste. Moreover, the use of zeolite to replace Portland cement resulted in a smaller amount of cement and thus caused a longer setting time to be observed. For the use of S, the reductions in the amount of cement and pozzolan resulted in an even smaller amount of cementing material and hence the setting times increased.

4.2.3. Compressive strength of the blended cement pastes

Table 4 shows the development of compressive strength in the cement paste in relation to the cement replacement level for the case of synthesized zeolites and natural zeolites. Concerning the use of SZ and NZ, replacement of 20% and 40% zeolites led to lower compressive strengths at all ages. It was observed that the compressive strengths of the cement pastes containing NZ were higher than those with SZ for the same replacement conditions and age, because more silica dioxide (the main component of nat-

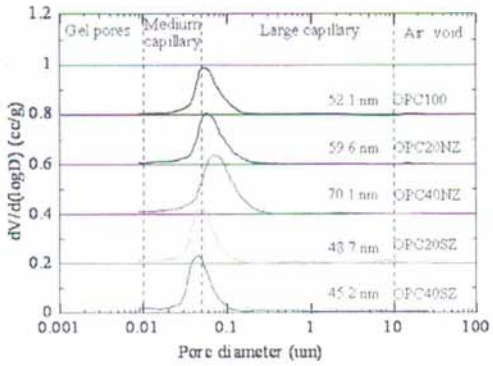

Fig. 5. Relationship between pore diameter and volume intruded of the blended cement pastes at 28 days.

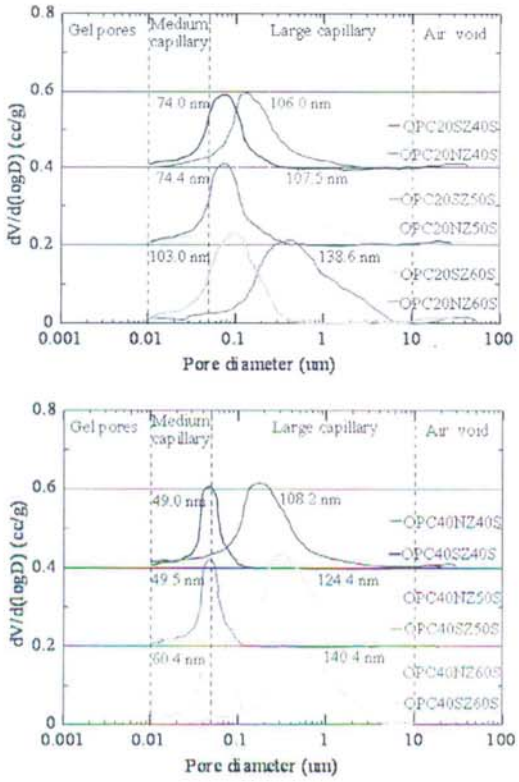

Fig. 6. Relationship between pore diameter and volume intruded of the solidified plating wastes using OPC, NZ and SZ as binders at 28 days.

ural zeolite) is contained than in the synthesized zeolites and cement. The pozzolanic activity of zeolite normally depends on the amount of the active amorphous phases of silica and alumina. As indicated in the XRD patterns in Fig. 3, the amount of the active amorphous phases of NZ is higher than that of SZ. The results of the compressive strengths of pastes OPC20SZ, OPC40SZ, OPC20NZ and OPC40NZ at 28 days of 31.1, 23.4, 62.4 and 50.7 MPa, respectively confirms the observation.

4.2.4. Compressive strength of pastes containing solidified plating waste

The experimental results showed that the rates of strength development in the solidified waste using SZ and NZ as solidification binders were higher than that with OPC. The composition of OPC hydration product is dominated by calcium silicate hydrate (C–S–H) which typically comprises 70–80% of the product (Deja, 2002). The metals may react with calcium hydroxide to produce insoluble compounds as a form of metal hydroxide; this mechanism inhibited the hydration and decreased the strength of the wastes, especially when the concentration of metal in the solidified waste was more than 0.3% by weight (Li et al., 2001; Asavapisit et al., 2001; Qin et al., 2003). The strength of these solidified wastes could be very low due to the inhibition of the cement reactions by the metal ions in the waste. Additionally, the strength of the solidified waste decreased when the amount of waste increased. For example, the strengths of pastes OPC20NZ40S, OPC20NZ50S, and OPC20NZ60S at 28 days were 57.3, 49.1 and 41.3 MPa, respectively. The results indicated that the plating sludge can be loaded in a proportion as high as 60 wt.% of the cement blended with 40 wt.% SZ and NZ at a 28-day compressive strength that meets the minimum requirement for disposal in a secure landfill (0.34 MPa).

4.2.5. Porosity and average pore diameter of blended cement pastes

The total porosity, capillary porosity and average pore diameter of the pastes at 7, 28 and 90 days are shown in Fig. 4. The incorporation of SZ and NZ increased the total porosity of the blended cement pastes as compared with the OPC paste at all ages. The total porosity increased with an increase in replacement by SZ and NZ. The increase in total porosity as a result of the utilization of zeolite was mainly due to the decrease in capillary porosity. Note that the compressive strength decreased, while the porosity of the blended cement paste increased (Poon et al., 2000; Isaia et al., 2003). The capillary porosity of the cement paste blended with NZ at all replacement levels decreased in comparison to that with SZ.

Fig. 4 shows the effect of the percent replacement of SZ and NZ on the average pore size in the cement pastes at age 7, 28 and 90 days. It can be observed that the average pore size of the additives decreased at the respective period of hydration because of the gradual filling of large pores by hydration products of cementitious materials; however, the extent of the decrease was variable. A greater decrease was observed for replacement by SZ, whereas the decrease was comparatively less for replacement by NZ. The average pore size tends to decrease as the percent replacement increases. The relationship between the pore diameter and incremental pore volume of the blended cement paste at 28 days is shown in Fig. 5. The critical pores sizes of the OPC100, OPC20NZ and OPC40NZ pastes were 52.1, 59.6 and 70.1 nm, respectively, and the pores were distributed as large capillary pores. The critical pores sizes of the OPC20SZ and OPC40SZ pastes were 48.7 and 45.2 nm, respectively, and these were distributed as medium capillary pores. These values were lower than that of the OPC100 paste. This suggests that the greater fineness of the zeolite was more effective in reducing the pore diameter of the paste. The results also showed that the blended cement paste containing zeolite presented a smaller pore size than the Portland cement paste. The pore size decreased with an increase in zeolite replacement. Similar results have also been reported in other studies (Poon et al., 1997, 1999a,b).

The relationship between the pore diameter and incremental pore volume of the solidified waste using OPC, SZ and NZ as binders at 28 days is shown in Fig. 6. The critical pore sizes of OPC20SZ40S, OPC20SZ50S and OPC20SZ60S were 74.0, 74.4 and 103.0 nm, respectively, and these pores were distributed as large capillary pores. Additionally, the critical pore sizes of the OPC40SZ40S, OPC40SZ50S and OPC40SZ60S pastes were 49.0, 49.5 and 60.4 nm, respectively. These results suggested that the increase in the amount of the plating waste resulted in increase in pore diameter of the paste. In contrast, the increase in the amount of SZ resulted in the decrease in the pore diameter of the paste.

As shown in Fig. 6, the critical pore sizes of OPC20NZ40S, OPC20NZ50S, OPC20NZ60S, OPC40NZ40S, OPC40NZ50S and OPC40NZ60S were 106.0, 107.5, 138.6, 108.2, 124.4 and 140.4 nm, respectively. These results suggested that as the amount of plating sludge increased, the pore diameter of the paste increased.

4.2.6. Fracture surface analysis byscanning electron microscopy (SEM)

The microstructure morphology of the fractured surface was determined by SEM for OPC100, OPC20SZ, OPC40SZ, OPC20NZ and OPC40NZ pastes at 28 days (see Fig. 7). The microstructure of OPC100 was porous and exhibited many voids, while OPC20SZ, OPC40SZ, OPC20NZ and OPC40NZ showed uniform and dense pastes. The incorporation of zeolites resulted in the increased hydration and pozzolanic reaction and thus reduced the pore sizes.

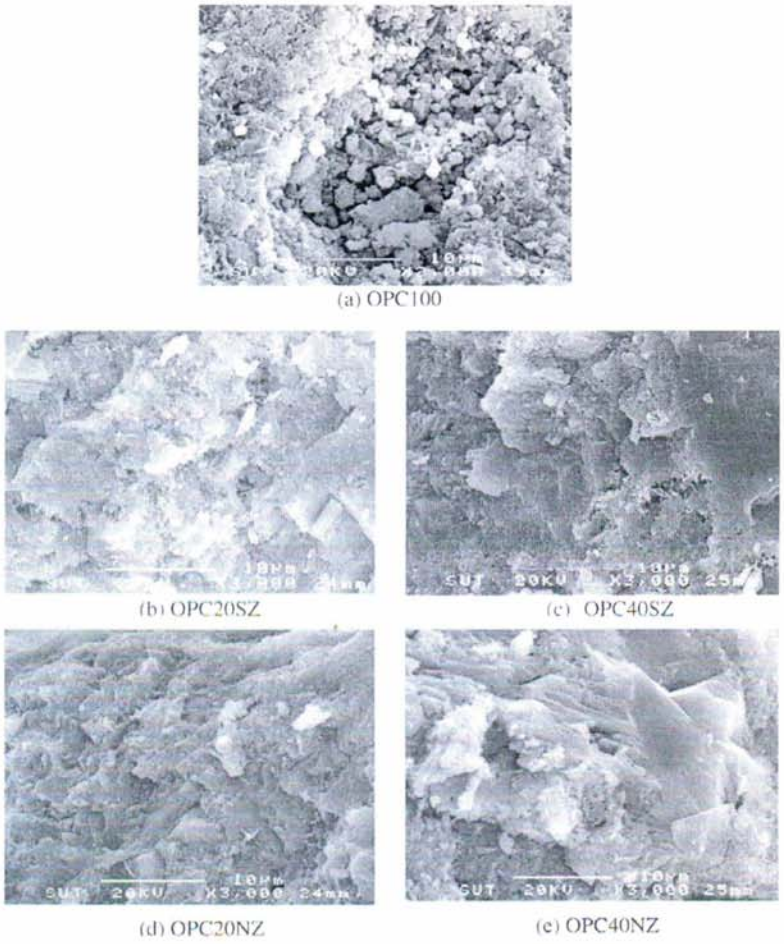

(a) OPC100

(b) OPC20SZ

(c) OPC40SZ

(d) OPC20NZ

(e) OPC40NZ

Fig. 7. Fracture surface of the blended cement pastes at 28 days.

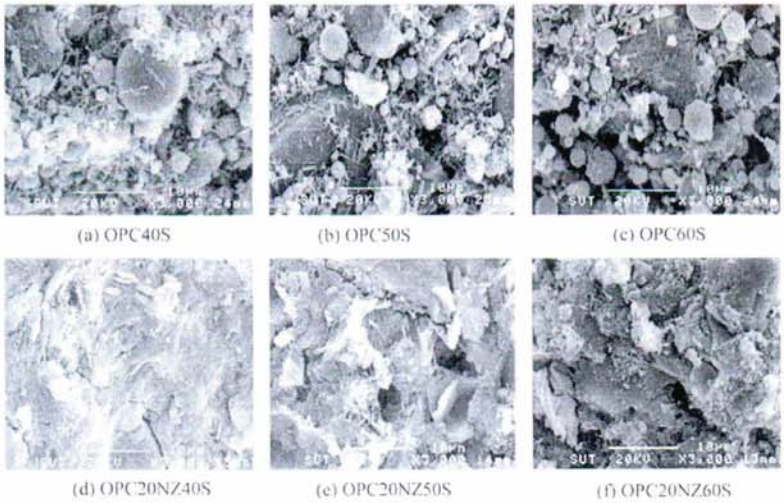

(a) OPC40S

(b) OPC50S

(c) OPC60S

(d) OPC20NZ40S

(e) OPC20NZ50S

(f) OPC20NZ60S

Fig. 8. Fracture surfaces of the solidified plating wastes at 28 days.

Table 5
Leachate pHs in TCLP leachates.

Sample	pH		
	Age 7 days	Age 28 days	Age 90 days
OPC100	6.3	6.5	6.6
OPC40S	6.4	6.6	6.7
OPC50S	7.1	7.2	7.2
OPC60S	7.7	7.7	7.7
OPC20SZ40S	7.6	7.5	7.4
OPC20SZ50S	7.9	7.9	7.8
OPC20SZ60S	7.8	7.9	7.9
OPC40SZ40S	9.8	9.5	9.5
OPC40SZ50S	8.8	8.8	8.7
OPC40SZ60S	8.5	8.5	8.6
OPC20NZ40S	11.4	11.5	11.5
OPC20NZ50S	11.2	11.2	11.2
OPC20NZ60S	11.1	11.1	11.1
OPC40NZ40S	11.2	11.1	11.1
OPC40NZ50S	10.8	10.8	10.9
OPC40NZ60S	9.7	9.6	9.6

Thus, replacing the Portland cement with some zeolites resulted in a dense paste.

Fig. 8 shows the fractured surfaces of the solidified plating waste at 28 days, as determined by SEM. The paste with more plating sludge showed a lower density because the proportion of binder in the mixture decreased. Because heavy metals inhibit hydration, the cement reaction was not completed, and some heavy metals did not react (Bishop et al., 2003). The replacement of Portland cement by zeolites showed a higher density than used Portland cement alone. The consequences of this are that the solidified waste was more porous, and the compressive strength of the solidified waste decreased significantly compared with those with the absence of plating sludge in the mixture.

4.2.7. Leaching analysis

Table 5 shows the leachate pH values in the TCLP leachates at 7, 28 and 90 days. The pH of the solution extracted from the solidified waste is increased from the initial pH. For example, the pH of pastes OPC100, OPC40S, OPC20SZ40S and OPC20NS40S pastes at 28 days were 6.5, 6.6, 7.5 and 11.5, respectively. The pH values increased because calcium hydroxide in the pores dissolved into the acid. Fig. 9 shows the metal concentrations in TCLP leachates, the results showed that the concentration of Cr in the leachate for all solidified waste samples was lower than the limit specified by the standards of the US EPA (<5.0 mg/l). It should be noted here that the untreated sludge also meets US EPA criteria for Cr. For example, the concentrations of Cr in the leachate of pastes

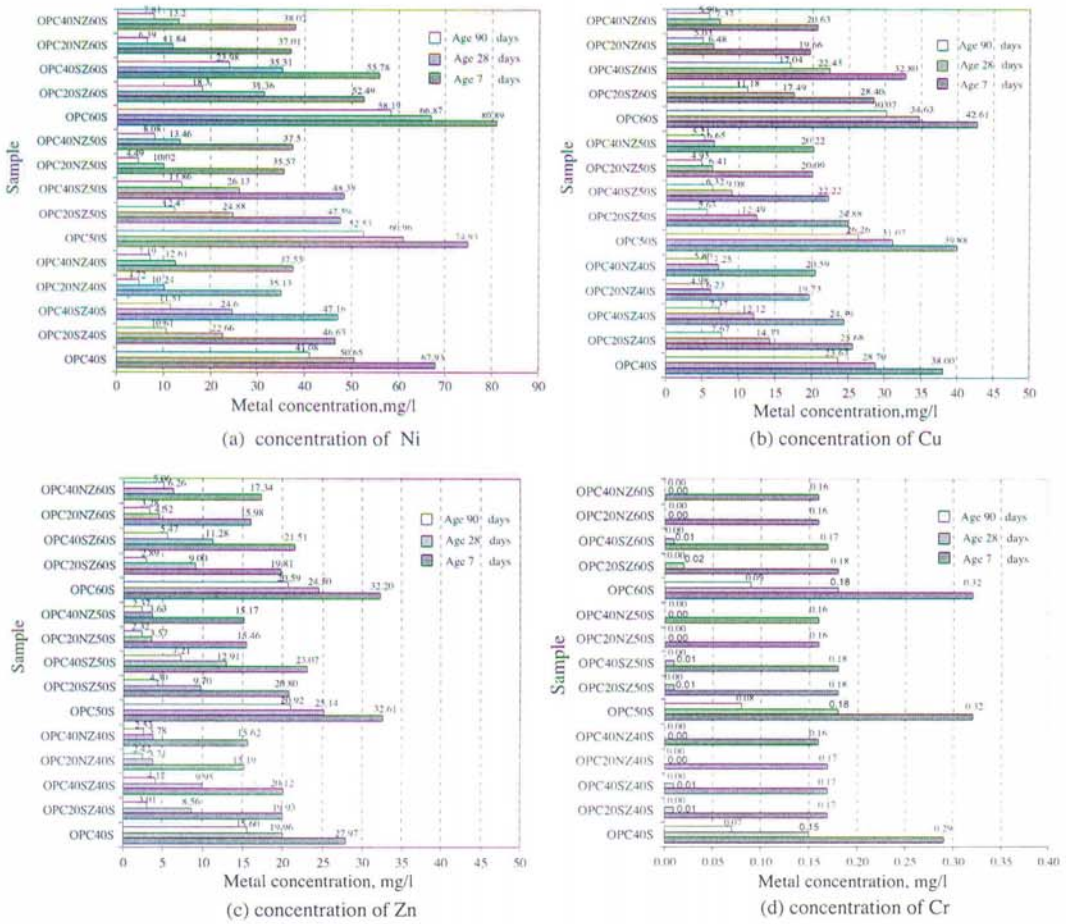

Fig. 9. Metal concentrations in TCLP leachates.

OPC20SZ40S, OPC20SZ50S, OPC20NZ40S and OPC20SZ50S at 7 days were 0.17, 0.18, 0.17 and 0.16 mg/l respectively. The Ni, Cu and Zn have no regulatory standards because these three metals are not classified as hazardous waste by the US EPA. The results showed that when sample age increased the effectiveness in reducing the leachability increased, For example, it was detected that OPC20NZ40S contained Ni of 35.13 mg/l at 7 days and this decreased to only 10.24 mg/l at 90 days. Using NZ as a binder effectively reduced leaching more than using SZ. For example, the concentrations of Ni in the leachate of pastes OPC40NZ40S and OPC40SZ40S at 28 days were 12.61 and 24.60 mg/l respectively. Additionally, the metal concentrations in the TCLP leachates that were extracted from the cement-based solidified plating waste were much lower than that extracted from the plating sludge. Effectiveness in reducing the leachability of solidified waste using SZ and NZ to replace OPC as a binder was higher than 80.0% at all ratios. This was because SZ and NZ mainly composed of SiO_2, Al_2O_3 and Fe_2O_3; and the structures of zeolites consist of three-dimensional frameworks of SiO_4 and AlO_4 tetrahedra. The aluminum ion is small enough to occupy the position in the center of the tetrahedron of four oxygen atoms, and the isomorphous replacement of Si^{4+} by Al^{3+} produces a negative charge in the lattice. The net negative charge is balanced by the exchangeable cation (Cheng and Bishop, 1992; Peralta et al., 1992). Thus, the effectiveness in reducing the leachability was higher using SZ and NZ than that with OPC alone. These results indicated that during the ion-exchange process, the metal ions had to move through the pores of zeolite mass and through channels of the lattice, and they had to replace exchangeable cations. The diffusion was fast through the pores, but was retarded when the ions moved through the smaller diameter channels. In this case, the metal ions uptake could mainly be attributed to the ion-exchange reactions in the microporous minerals of zeolite (Erdem et al., 2004).

5. Conclusions

On the basis of the results of this study, the following conclusions can be drawn.

1. The blended cement pastes containing synthesized zeolite and natural zeolite exhibited higher total porosity and capillary porosity than those containing Portland cement alone. This resulted in the lower compressive strengths of blended cement pastes compared to that of the control Portland cement paste.
2. The pore size distribution and the average pore diameter of the blended cement paste containing zeolites decreased with an increase in zeolite content which resulted in the dense structure of the paste. This effect was caused by the hydration reaction and the pozzolanic reaction.
3. The use of zeolites to partially replace Portland cement as a solidification binder produced solidified waste with lower strength. However, it is more effectiveness in terms of leachablity than the use of Portland cement alone.
4. The application of natural zeolite as a binder with Portland cement to reduce the leaching of heavy metals resulted in a better outcome than using synthetic zeolites with cement, or cement alone. The use of natural zeolite with Portland cement as a binder to solidify waste sludge is appropriate as the leachablity was reduced and the compressive strength complied with the US EPA standard.

Acknowledgments

The authors would like to acknowledge the financial support by the Higher Education Research Promotion and National Research University Project of Thailand, Office of the Higher Education Commission, through the Advanced Functional Materials Cluster of Khon Kaen University, and the Strategic Scholarships for Frontier Research Network for the Joint Ph.D. Program, Thai Doctoral degree. Thanks are also extended to the Thailand Research Fund (TRF) for financial support under the TRF Senior Research Scholar, Grant No. RTA5480004 and the TRF New Researcher Scholar, Grant No. MRG5280178.

References

Asavapisit, S., Nanthamontry, W., Polprasert, C., 2001. Influence of condensed silica fume on the properties of cement-based solidified wastes. Cement and Concrete Research 31, 1147–1152.

Asavapisit, S., Naksrichum, S., Harnwajanawong, N., 2005. Strength, leachability and microstructure characteristics of cement-based solidified plating sludge. Cement and Concrete Research 35, 1042–1049.

Bishop, M., Bott, S.G., Barron, A.R., 2003. A new mechanism for cement hydration inhibition: solid-state chemistry of calcium nitrilotris(methylene)-triphosphonate. Chemistry of Materials 15 (16), 3073–3088.

Cheng, K.Y., Bishop, P.L., 1992. Metals distribution in solidified/stabilized waste forms after leaching. Hazardous Waste and Hazardous Materials 9, 163–312.

Chindaprasirt, P., Jaturapitakkul, C., Sinsiri, T., 2005. Effect of fly ash fineness on compressive strength and pore size of blended cement paste. Cement and Concrete Composites 27, 425–428.

Chindaprasirt, P., Jaturapitakkul, C., Sinsiri, T., 2007. Effect of fly ash fineness on microstructure of blended cement paste. Construction and Building Materials 21, 1534–1541.

Deja, J., 2002. Immobilization of Cr^{6+}, Cd^{2+}, Zn^{2+} and Pb^{2+} in alkali-activated slag binder. Cement and Concrete Research 32, 1971–1979.

Erdem, E., Karapinar, N., Donat, R., 2004. The removal of heavy metal cations by natural zeolites. Journal of Colloid and Interface Science 280, 309–314.

Feng, N.-Q., Peng, G.-F., 2005. Applications of natural zeolite to construction and building materials in China. Construction and Building Materials 19, 579–584.

Feng, N.-Q., Xing, F., Leng, F.-G., 2000. Zeolite ceramsite cellular concrete. Magazine of Concrete Research 52, 117–122.

Isaia, G.C., Gastaldini, A.L.G., Moraes, R., 2003. Physical and pozzolanic action of mineral addition on the mechanical strength of high-performance concrete. Cement and Concrete Research 25, 69–76.

Li, X.D., Poon, C.S., Sun, H., Lo, I.M.C., Kirk, D.W., 2001. Heavy metal speciation and leaching behaviours in cement based solidified/stabilized waste materials. Journal of Hazardous Materials A 82, 215–230.

Peralta, G.L., Ballsteros, F.C., Cepeda, M.L., 1992. Treatment and Disposal of Heavy Metal Waste Using Cementitious Solidification. Nation Engineering Center, Philippines, pp. 2–37.

Poon, C.S., Wong, Y.L., Lam, L., 1997. The influence of different curing conditions on the pore structure and related properties of fly ash cement pastes and mortars. Construction and Building Materials 11, 383–393.

Poon, C.S., Lam, L., Kou, S.C., Lin, Z.S., 1999a. A study on the hydration rate of natural zeolite blended cement paste. Construction and Building Materials 13, 427–432.

Poon, C.S., Lam, L., Wong, Y.L., 1999b. Effect of fly ash and silica fume on interfacial porosity of concrete. ACI Material Journal, 197–205.

Poon, C.S., Lam, L., Wong, Y.L., 2000. A study on high strength concrete prepared with large volume of law calcium fly ash. Cement and Concrete Research 30, 447–455.

Qin, G., Sun, D.D., Tay, J.H., 2003. Characterization of mercury- and zinc-doped alkali-activated slag matrix Part II. Zinc. Cement and Concrete Research 33, 1257–1262.

Quanlin, N., Naiqian, F., 2005. Effect of modified zeolite on expansion of alkaline silica reaction. Cement and Concrete Research 35, 1784–1788.

3. Sinsiri, T.*, Phoo-ngernkham, T., Sata V., Chindaprasirt, P., 2012, The effect of replacement fly ash with diatomite in geopolymer mortar, Computer and Concretes, Vol. 9, No.6, pp. 427-437. (IF= 0.763)

Computers and Concrete, Vol. 9, No. 6 (2012) 427-437

The effects of replacement fly ash with diatomite in geopolymer mortar

Theerawat Sinsiri*[1], Tanakorn Phoo-ngernkham[1], Vanchai Sata[2] and Prinya Chindaprasirt[2]

[1]*School of Civil Engineering, Institute of Engineering, Suranaree University of Technology, Nakhonratchasima 30000, Thailand*

[2]*Sustainable Infrastructure Research and Development Center, Dept. of Civil Engineering, Faculty of Engineering, Khon Kaen University, Khon Kaen 40002, Thailand*

(Received April 7, 2011, Revised July 29, 2011, Accepted August 22, 2011)

Abstract. This article presents the effect of replacement fly ash (FA) with diatomite (DE) on the properties of geopolymer mortars. DE was used to partially replace FA at the levels of 0, 60, 80 and 100% by weight of binder. Sodium silicate (Na_2SiO_3) and sodium hydroxide (NaOH) solutions were used as the liquid portion in the mixture in order to activate the geopolymerization. The NaOH concentrations of 15M, Na_2SiO_3/NaOH ratios of 1.5 by weight, and the alkaline liquid/binder (LB) ratios by weight of 0.40, 0.50, 0.60 and 0.70 were used. The curing at temperature of 75°C for 24 h was used to accelerate the geopolymerization. The flows of all fresh geopolymer mortars were tested. The compressive strengths and the stress-strain characteristics of the mortar at the age of 7 days, and the unit weights were also tested. The results revealed that the use of DE to replace part of FA as source material in making geopolymer mortars resulted in the increased in the workability, and strain capacity of mortar specimens and in the reductions in the unit weights and compressive strengths. The strain capacity of the mortar increased from 0.0028 to 0.0150 with the increase in the DE replacement levels from 0 to 100%. The mixes with 15M NaOH, Na_2SiO_3/NaOH of 1.5, LB ratio of 0.50, and using 75°C curing temperature showed 7 days compressive strengths 22.0-81.0 MPa which are in the range of normal to high strength mortars.

Keywords: geopolymer; diatomite; workability; compressive strength; strain capacity.

1. Introduction

Portland cement concrete is a mixture of Portland cement, water and aggregates. Nowadays, concrete is the most used construction material. However, the process of manufacturing of Portland cement consumes a large amount of energy and as a result releases a very large amount of green house gas to the atmosphere. The use of by-products or natural binders as cement replacement can, therefore, reduce the consumption of cement in concrete work. In the last decade, geopolymer binders have emerged as one of the possible alternative to cement binders for applications in concrete industry. Geopolymer is an inorganic binder material and can be produced by a polymeric reaction of alkali activating solution with silica and alumina in source material from geological origin or pozzolanic materials such as metakaolin, fly ash (FA) and rice husk ash (Davidovits 1991). The geopolymer mortar and concrete possess similar strength and appearance to those of normal

* Corresponding author, Ph.D., E-mail: sinsiri@sut.ac.th

Portland cement. Their mechanical properties, fire resistance and acid resistance are superior to those of normal Portland mortar and concrete (Palomo *et al.* 1999, Hardjito and Rangan 2005).

Diatomite (DE) or diatomaceous earth is a sedimentary deposit with origin from sedimentation of single cell seaweeds. It is light in weight due to high porosity and is relatively attractive in dark-yellow shade due to high content of ferrous compound and semi-crystalline siliceous phase (Owen and Utha-aroon 1999). The particle size is therefore quite fine with cellular surface consisting of micro-pores (Antonides 1999). DE has been used as a good source material for lightweight brick, heavy metals removal and absorbent agent in wastewater treatment process (Pimraksa and Chindaprasirt 2009, Elden *et al.* 2010). The deposit of DE or diatomaceous earth clay in Lampang province in the north of Thailand is quite large with estimation at more than 100 million tons. The mineral composition consists primarily of silica with some alumina and ferrous oxide (Sierra *et al.* 2010). It is a pozzolan and should, therefore, be suitable source material for making geopolymer.

The annual output of lignite FA from Mae Moh power station in the North of Thailand is around 3 million tons. This FA consists mainly of SiO_2, Al_2O_3, Fe_2O_3 and CaO and some impurities. The use of fly ash as pozzolan in concrete is constantly increasing because it improves the properties of concrete, namely workability, durability and long term strength in hardened concrete (Rukzon and Chindaprasirt 2008, Yeh 2008). In addition, it has also been shown to be suitable as a source material for making good geopolymer (Chindaprasirt *et al.* 2007).

This research aims to study the preparation of FA and DE geopolymer. The DE could be used for the adjustment of the silica content in the mixture. The knowledge of the use of high calcium lignite FA and silica rich DE in producing geopolymer would be beneficial to the understanding and to the future applications of the materials.

2. Experimental details

2.1 Materials

Lignite fly ash (FA) from Mae Moh power station and raw DE from Lumpang in the north of Thailand, sodium hydroxide (NaOH), and sodium silicate (Na_2SiO_3) with 15.32% Na_2O, 32.87% SiO_2 and 51.81% H_2O were the materials used. The raw DE was calcined at 800°C for 6 hours in order to improve its characteristics. (Yilmaz and Ediz 2008, Zuhua *et al.* 2009). The 6 hours calcination was used since the shorter period was found to be insufficient as the calcined products was still not properly burnt. For longer calcination, the formation of crystal could be detected. In addition, tap water and local river sand with specific gravity of 2.69 were used for making geopolymer mortar. In order to minimize the effect of the liquid absorption of fine aggregate, the sand in saturated surface condition was used.

The chemical composition and physical properties of materials are given in Tables 1 and 2, respectively. The SiO_2+Al_2O_3+Fe_2O_3 content of the FA is 81.01% and the CaO content is high at

Table 1 Chemical composition of materials (by weight)

Materials	SiO_2	Al_2O_3	Fe_2O_3	CaO	MgO	K_2O	Na_2O	TiO	SO_3	LOI
FA	43.87	26.33	10.81	12.69	1.23	1.10	-	-	2.74	1.23
DE	59.30	10.00	18.50	1.20	0.46	1.98	0.20	0.23	0.02	8.10

Table 2 Physical properties of materials

Physical properties	FA	DE	Sand
Specific gravity	2.41	2.33	2.69
Bulk density (kg/m^3)	973	490	1625
Median particle size (μm)	17.6	18.3	-
Blaine fineness (cm^2/g)	4300	12600	-

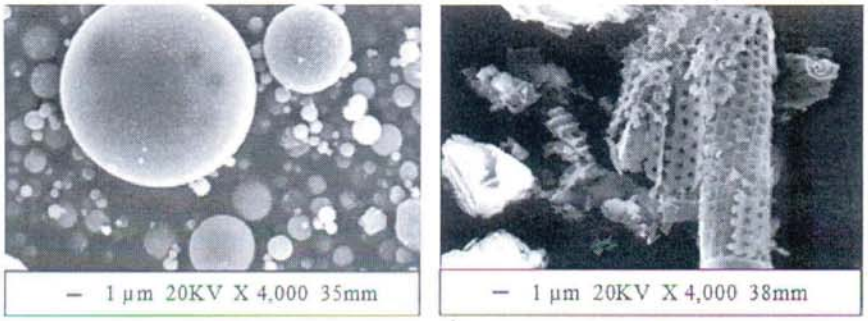

(a) FA (b) DE

Fig. 1 The scanning electron micrographs of FA and DE

12.69% which is typical of the lignite FA. The DE consists of 59.30% SiO_2, 10.00% Al_2O_3 and 18.50% Fe_2O_3. FA has a mean particle size of 17.6 μm, a Blaine fineness of 4300 cm^2/g and a specific gravity of 2.41. DE has a mean particle size of 18.3 μm, a Blaine fineness of 12600 cm^2/g. Fig. 1 shows the scanning electron micrographs (SEM) of FA and DE. The FA particles are spherical and smooth in the surface while the DE particles consist of cellular porous particles with some small irregular shape plate-like particles.

2.2 Mix proportion and testing

All geopolymer mortars were made with sand to binder (FA+DE) ratio of 1.50. The FA100, FADE60, FADE80 and FADE100 mortars with corresponding FA:DE ratios of 100:0, 40:60, 20:80 and 0:100 were the mixes used. In addition, the effects of the *L/B* ratios on properties of geopolymer mortars were also studied.

The mixing was done in an air conditioned room at approximately 25°C to eliminate the possible effect of temperature variation. The NaOH and Na_2SiO_3 solutions were mixed before the start of the mixing. FA and DE were thoroughly mixed until the mixture was homogenous. Sand was incorporated into the blend of FA and DE and mixed for 1 minute. The prepared NaOH and Na_2SiO_3 solution was added and mixed for another 10 minutes. Right after the mixing, the flow values of fresh geopolymer mortar were the average of three samples and were tested in accordance with ASTM C 1437 (2003).

The fresh mortar was cast into 50 × 50 × 50 mm^3 cube moulds. The specimens were compacted in two layers and tamping as described in the ASTM C 109 (2003). The specimens were immediately wrapped with vinyl sheet to protect moisture loss and kept in the controlled room at 25°C. The specimens were then placed in the oven for heat curing at 75°C for 24 hours. After the heat curing,

the specimens were put in the laboratory to cool down. They were demoulded the next day and kept in the control room. The compressive strengths of mortars were the average of three samples and were determined in accordance with ASTM C 109 (2003).

3. Results and discussions

3.1 Workability of geopolymer mortar

Fig. 2 shows the relationship between flow of geopolymer mortar and LB ratios at various replacement levels of DE. At low LB ratio, the geopolymer mortars were very stiff with low flow values between 2-16% for the LB ratio of 0.40 mortars. The workability of the mixes also increased with the increase the LB ratio. For example, the workable mortars with flow value of 85-126% were obtained with the LB ratio of 0.70. This result conforms to the previous research (Sathonsaowaphak *et al.* 2009) which explained that an increase in fluid medium content resulted in less particle interaction and increased the workability of the mixture. At the same LB ratio, the replacement FA with DE also increased the workability of mortar. At the LB ratio of 0.60, the flow of FA100, FADE60, FADE80 and FADE100 were 53, 82, 108 and 96%, respectively. The increasing of workability in mortar containing DE may be due to the low bulk density of DE as comparing with FA. The result also conformed to Torres and Garcia-Ruiz (2009) report that the use of lightweight pozzolan in cement mortar could be improved workability of mortar.

The empirical equations could be expressed for the workable geopolymer mortar with flow value (F) in terms of LB ratio with DE content of 0, 60, 80 and 100% as follows

For

$$\text{DE}=0\%,\ F=267.47(\text{LB})-103.35,\ (R^2=0.99) \quad (1)$$

$$\text{DE}=60\%,\ F=334.65(\text{LB})-120.05,\ (R^2=0.95) \quad (2)$$

$$\text{DE}=80\%,\ F=353.59(\text{LB})-116.26,\ (R^2=0.95) \quad (3)$$

$$\text{DE}=100\%,\ F=345.72(\text{LB})-110.21,\ (R^2=0.83) \quad (4)$$

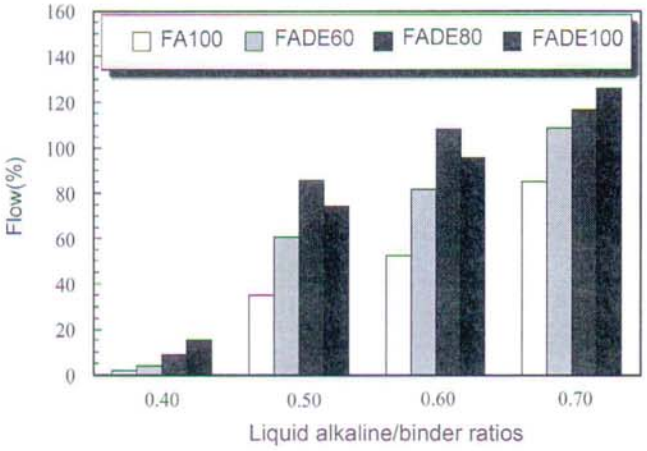

Fig. 2 Flows of geopolymer mortar with various LB ratios

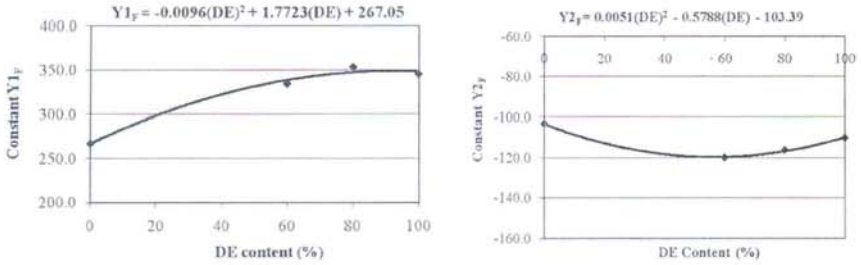

(a) Constant $Y1_F$ (b) Constant $Y2_F$

Fig. 3 Relationship between constants $Y1_F$, $Y2_F$ and DE contents

The relationships of the flow value (F) and liquid alkaline/binder ratio (LB) in Eqs. (1)-(3) and (4) could be written as Eq. (5)

$$F = Y1_F(\mathrm{LB}) + Y2_F \tag{5}$$

Where

$$Y1_F = -0.0096(\mathrm{DE})^2 + 1.7723(\mathrm{DE}) + 267.05, \quad (R^2 = 0.99)$$

$$Y2_F = 0.0051(\mathrm{DE})^2 - 0.5788(\mathrm{DE}) - 103.39, \quad (R^2 = 0.99)$$

F = flow value of geopolymer mortar (%)
DE = amount of DE between 0 to 100%
LB = liquid alkaline/binder ratio between 0.40 to 0.70

The constants $Y1_F$ and $Y2_F$ were obtained by curve fitting of the results from Fig. 3 for DE content of 0, 60, 80 and 100%. The results of workability in term of flow from this equation were compared to the actual test results as shown in Fig. 4. The relationship in Eq. 5 is, therefore, useful to predict the flow of geopolymer mortar at various LB ratio and amount of replacement FA with DE. The non-linear behavior of flow of FADE80 and FADE100 mixes were due to the large

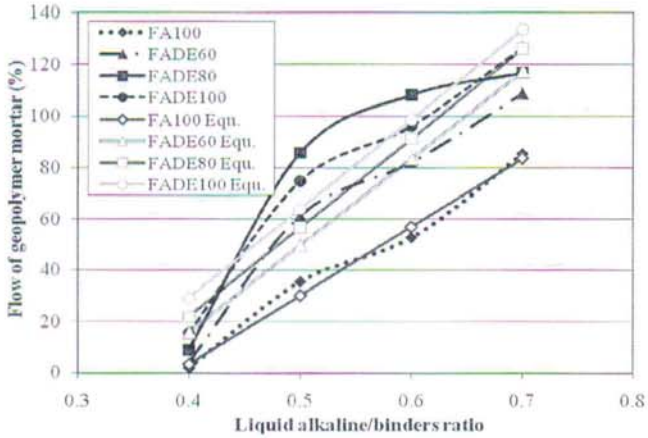

Fig. 4 Comparison of the flows of geopolymer mortar obtained from Eq. 5 and from experiment

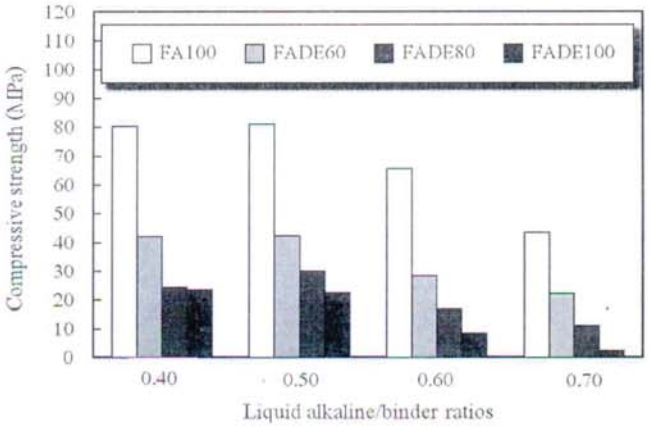

Fig. 5 Compressive strength of geopolymer mortar with various LB ratios

improvement of flow with high contents of DE of 80 and 100%. At 0.5 LB ratio, the large improvements of flow were obtained as a result of the large content of DE and an increase in the LB ratio. For higher LB ratios of 0.6 and 0.7, the small increases in the flow were obtained as they were approaching the obtainable maximum slump values.

3.2 The compressive strength of geopolymer mortar

The effect of LB ratios on 7 days compressive strength of geopolymer mortar at various DE contents is shown in Fig. 5. At the LB ratios of 0.40 and 0.50, the compressive strengths of the two series were almost the same. When the LB ratio was increased to 0.6 and 0.70, the compressive strengths of mortar decreased. For example, the 7 days compressive strength of FADE60 mortar at LB ratios of 0.40, 0.50, 0.60 and 0.70 were 42, 42, 28 and 22 MPa, respectively. Since, at high LB ratios may be due to excess of OH^- concentration in the mixture which decreased mortar compressive strength (Hardjito *et al.* 2008). In addition, Barbosa *et al.* (1999) indicated that the excess liquid solution could disrupt the polymerization process. The result also conformed to Sathonsaowaphak *et al.* (2009) report that the compressive strength of bottom ash geopolymer mortar seemed to decrease at high LB ratio (0.45-0.71).

The replacements of FA with DE in geopolymer mortar exhibited to decrease the compressive strength. At the LB ratio of 0.50, the 7 days compressive strengths of FA100, FADE60, FADE80 and FADE100 mortars were 81, 42, 30 and 22 MPa, respectively. This was due to the replacements of FA with DE caused to higher the SiO_2/Al_2O_3 ratios in the mixtures. From the chemical composition of FA and DE in this study, FA100, FADE60, FADE80 and FADE100 mortars had the SiO_2/Al_2O_3 ratio of 1.7, 4.2, 5.0 and 5.9, respectively. The suitable SiO_2/Al_2O_3 ratio for relatively high compressive strength geopolymer was around 1.9 (Duxson *et al.* 2005). In addition, many researchers (Duxson *et al.* 2005, Wongpa *et al.* 2010, Nazari *et al.* 2011) found that the SiO_2/Al_2O_3 ratio is the major parameter to control goepolymer matrix properties and at higher SiO_2/Al_2O_3 ratio resulted in low compressive strength.

The empirical equations could be expressed for the compressive strengths (C) of geopolymer mortars in terms of LB ratio and DE contents as follows

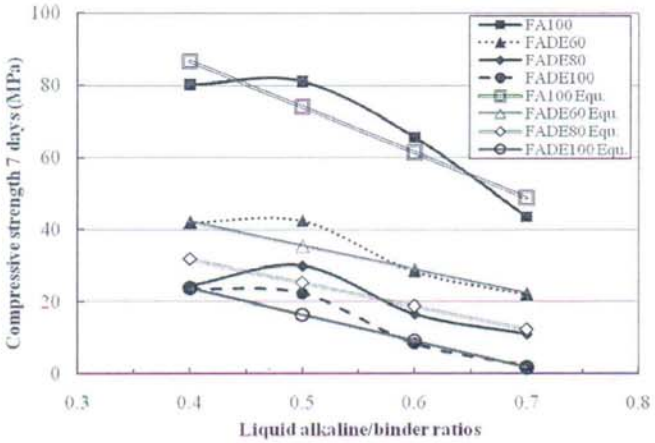

Fig. 6 Comparison of the 7 days compressive strengths of geopolymer mortars obtained from Eq. 6 and from experiment

$$C = Y1_C(\mathrm{LB}) + Y2_C \tag{6}$$

Where

$$Y1_C = -0.0117(\mathrm{DE})^2 + 1.6961(\mathrm{DE}) - 125.99, \quad (R^2 = 0.92)$$

$$Y2_C = 0.0075(\mathrm{DE})^2 - 1.5879(\mathrm{DE}) + 136.93, \quad (R^2 = 0.98)$$

C = compressive strength of geopolymer mortar (MPa)
DE = amount of DE between 0 to 100%
LB = liquid alkaline/binder ratio between 0.40 to 0.70

The 7 days compressive strengths from this equation were compared to the actual test result as shown in Fig. 6. The relationship in Eq. (6) is, therefore, useful to predict the 7 days compressive strength of geopolymer mortar at various LB ratios and amounts of replacement FA with DE.

3.3 The unit weight of geopolymer mortar

The unit weight FA and DE geopolymer mortar is shown in Fig. 7. It was found that the increasing LB ratio from 0.40 to 0.70 seemed to decrease the unit weight of mortar and the incorporation DE in the mixture decreased the unit weight of mortar. The FA100 (0% DE) mortars had unit weight range from 2180 to 2280 kg/m^3 and the use of 100% DE in geopolymer mortar (FADE100 mortar) reduced the unit weight to 1990 to 2100 kg/m^3. The reason is the low bulk density and high porosity of DE as compare to FA. Hence, at high LB ratio and the characteristic of DE can apply for lightweight geopolymer matrix.

The empirical equations of the unit weights geopolymer mortar (W) in terms of LB ratio and DE contents could be drawn as follows

$$W = Y1_W(\mathrm{LB}) + Y2_W \tag{7}$$

Where

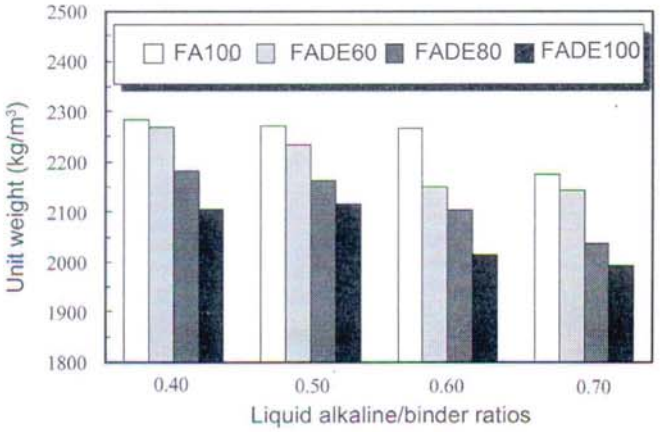

Fig. 7 Unit weights of geopolymer mortars with various of LB ratios

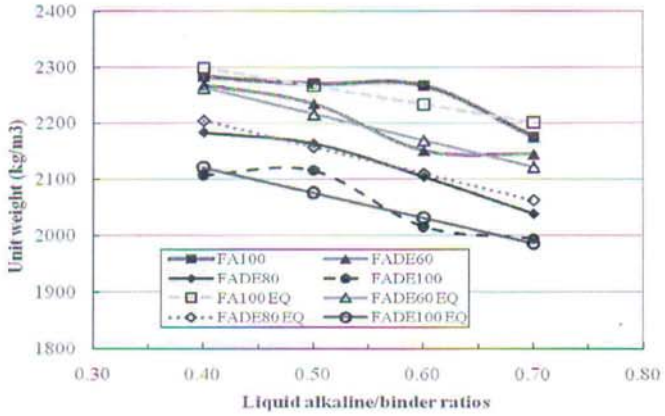

Fig. 8 Comparison the unit weight of geopolymer mortar obtained from Eq. (15) and from experiment

$$Y1_W = 0.0305(\mathrm{DE})^2 - 4.282(\mathrm{DE}) - 326.73, \quad (R^2 = 0.94)$$

$$Y2_W = -0.0419(\mathrm{DE})^2 + 2.9034(\mathrm{DE}) + 2429.3, \quad (R^2 = 1.00)$$

W = unit weight of geopolymer mortar (kg/m^3)
DE = amount of DE between 0 to 100%
LB = liquid alkaline/binder ratio between 0.40 to 0.70

Fig. 8 shows the unit weight of geopolymer mortar from Eq. (7) and the actual test results. It was found this equation is useful to predict the unit weight of geopolymer mortar at various LB ratios and amounts of replacement FA with DE.

3.4 The stress-strain characteristic of geopolymer mortar

The relationship between stress and strain of geopolymer mortars with the Na_2SiO_3/15 M NaOH

ratio at 1.5 and the LB ratio of 0.50 at 7 days is shown in Fig. 9. The cord elasticity modulus was calculated as described in the ASTM C 469 (2003). The value of elastic modulus increased with the increase in compressive strength, which was similar to plain concrete. The replacement FA with DE reduced the compressive strength and the elastic modulus owing to an increase in the SiO_2/Al_2O_3 ratio (Pacheco-Torgal *et al.* 2008). However, the strain at peak stress (strain capacity) seemed to increase with DE content. Hence, the FA based geopolymer mortar mixes with DE exhibited a more deformable behavior. This reason is probably due to the high porosity and low bulk density of DE. The 7 days elastic modulus of FA100, FADE60, FADE80 and FADE100 mortars were 28.3, 12.0, 7.2 and 3.2 GPa with the strain at peak stress of 0.0028, 0.0047, 0.064 and 0.015, respectively.

Fig. 10 shows the relationship between modulus of elasticity and the compressive strength of geopolymer mortar. It was observed that the modulus of elasticity tended to increase linearly to the square root of compressive strength. The equation predicting this relationship can be drawn as follows

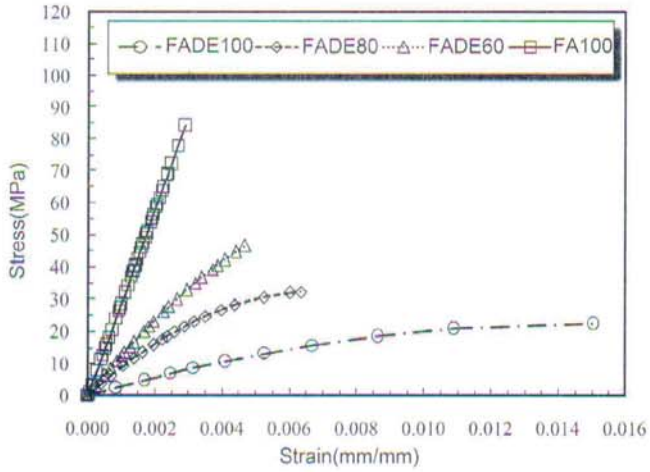

Fig. 9 Relationship between stress and strain of geopolymer mortar

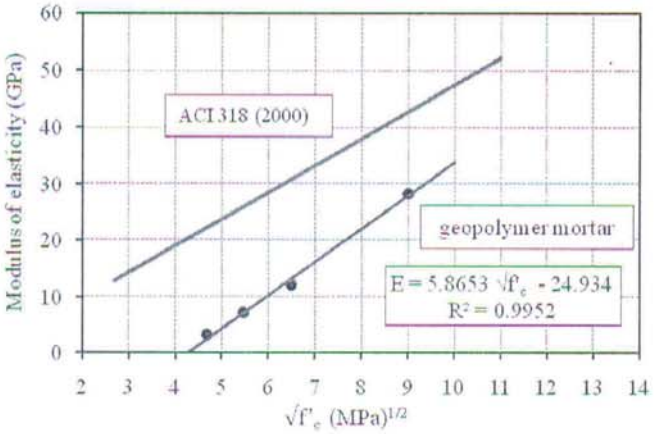

Fig. 10 Modulus of elasticity of geopolymer mortars

$$E = 5.8653\sqrt{f_c'} - 24.934 \quad (8)$$

Where

E = modulus of elasticity (GPa)
f_c' = compressive strength (MPa)

The values of modulus of elasticity in this study were lower than those predicted by ACI 318 (2000). The same trend of result was also reported by Wongpa *et al.* (2010) from the study of the compressive strength, modulus of elasticity and water permeability of inorganic polymer concrete. The increase in the strain capacity with the increase in the DE content is very useful in terms of the improvement in the cracking of this inorganic polymer matrix.

4. Conclusions

Based on the obtained data, it can be concluded that the DE could be used in conjunction with FA to produce good geopolymer mortars with improved workability, strain capacity and reduced unit weight of mortar. The use of DE to replace part of FA as source material in making geopolymer mortars resulted in an improvement in the workability of mortar. The compressive strength and modulus of elasticity of geopolymer mortar decreased with an increase in the DE content as a result of the increase in the SiO_2/Al_2O_3 ratio. The mixes with 15M NaOH, Na_2SiO_3/NaOH of 1.5, LB ratio of 0.50 and using 75°C curing temperature showed 7 days compressive strengths of 22.0-81.0 MPa. The strain capacity of the mortar, however, increased from 0.0028 to 0.0150 with the increase in the DE replacement. In addition, the incorporation DE in the mixture decreased the unit weight of mortar. The improvement in the workability, strain capacity and unit weight with the incorporation of DE can be used to advantageous in designing the geopolymer mortars using these based materials.

Acknowledgements

The authors would like to acknowledge the financial support by the Higher Education Research Promotion and National Research University Project of Thailand, Office of the Higher Education Commission, through the Advanced Functional Materials Cluster of Khon Kaen University. Thanks are also extended to the Thailand Research Fund (TRF) under the TRF New Researcher Scholar, and grant No. MRG5280178, the National Research Council of Thailand.

References

ACI 318 (2000), *Building code requirement for structure concrete practice*, ACI 318M-95. American Concrete Institute Part 3.

ASTM C 109 (2003), *Standard test method for compressive strength of hydraulic cement mortar*, ASTM C 109/C 109M-2, Annual Book of ASTM Standard.

ASTM C 150 (2003), *Standard specification for portland*, ASTM C 150-02a, Annual Book of ASTM Standard.

ASTM C 469 (2003), *Standard test method for static modulus of elasticity and poisson's ratio of concrete in compression*, ASTM C 469-02, Annual Book of ASTM Standard.

ASTM C 1437 (2003), *Standard test method for flow of hydraulic cement mortar*, ASTM C 1437-01, Annual Book of ASTM Standard.

Antonides, L.E. (1999), Diatomite: U.S. Geological Survey Mineral commodity summaries 1, 60-61.

Barbosa, V.F.F., MacKenzie, K.J.D. and Thaumaturgo, C. (1999), "Synthesis and characterization of sodium polysialate inorganic polymer based on alumina and silica", Davidovits J, Davidovits R, James C. (Eds.), *Proceeding of the Second International Conference on Geopolymer-GEOPOLYMER'99*, France.

Chindaprasirt, P., Chareerat, T. and Sirivivananon, V. (2007), "Workability and strength of coarse high calcium fly ash geopolymer", *Cement Concrete Comp.*, **29**(3), 224-229.

Davidovits, J. (1991), "Geopolymer: inorganic polymeric new materials", *J. Therm. Anal.*, **37**(8), 1633-1656.

Duxson, P., Provis, J.L., Lukey, G.C., Mallicoat, S.W., Kriven, W.M. and Van Deventer, J.S.J. (2005), "Understanding the relationship between geopolymer composition, microstructure and mechanical properties", *Colloid. Surface. A.*, **269**(1-3), 47-58.

Elden, H., Morsy, G. and Bakr, M. (2010), "Diatomite: it characterization, modifications and applications", *Asian J. Mater. Sci.*, **2**(3), 121-136.

Hardjito, D., Cheak, C.C. and Ing, C.H.L. (2008), "Strength and setting time of low calcium fly ash-based geopolymer mortar", *Mod. Appl. Sci.*, **2**(4), 3-11.

Hardjito, H. and Rangan, R.V. (2005), *Development and properties of low-calcium fly ash based geopolymer concrete*, Research report GC1. Perth, Australia: Faculty of Engineering, Curtin University of Technology.

Jumrat, S., Chatveera, B. and Rattanadecho, P. (2011), "Dielectric properties and temperature profile of fly ashbased geopolymer mortar", *Int. Commun. Heat Mass*, **38**(2), 242-248.

Nazari, A., Bagheri, A. and Riahi, S. (2011), "Properties of geopolymer with seeded fly ash and rice husk bark ash", *Mater. Sci. Eng. A.*, **528**(24), 7395-7401.

Owen, R.B. and Utha-aroon, C. (1999), "Diatomaceous sedimentation in the tertiary lampang basin, northern Thailand", *J. Paleolimnol.*, **22**(1), 81-95.

Pacheco-Torgal, F., Castro-Gomes, J. and Jalali, S. (2008), "Properties of tungsten mine waste geopolymeric binder", *Constr. Build. Mater.*, **22**(6), 1201-1211.

Palomo, A., Grutzeck, M.W. and Blanco, M.T. (1999), "Alkali-activated fly ashes: A cement for the future", *Cement Concrete Res.*, **29**(8), 1329-1329.

Pimraksa, K. and Chindaprasirt, P. (2009), "Lightweight bricks made of diatomaceous earth, lime, and gypsum", *Ceram. Int.*, **35**(1), 471-478.

Rukzon, S. and Chindaprasirt, P. (2008), "Mathematical model of strength and porosity of ternary blend Portland rice husk ash and fly ash cement mortar", *Comput. Concrete*, **5**(1), 75-88.

Sathonsaowaphak, A., Chindaprasirt, P. and Pimraksa, K. (2009), "Workability and strength of lignite bottom ash geopolymer mortar", *J. Hazard Mater.*, **168**(1), 44-50.

Sierra, E.J., Miller, S.A., Sakulich, A.R., MacKenzie, K. and Barsoum, M.W. (2010), "Pozzolanic activity of diatomaceous earth", *J. Am. Ceram. Soc.*, **93**(10), 3406-3410.

Torres, M.L. and Garcia-Ruiz, P.A. (2009), "Lightweight pozzolanic materials used in mortars: Evaluation of their influence on density, mechanical strength and water absorption", *Cement Concrete Comp.*, **31**(2), 114-119.

Wong, J., Kiattikomol, K., Jaturapitakkul, C. and Chindaprasirt, P. (2010), "Compressive strength, modulus of elasticity, and water permeability of inorganic polymer concrete", *Mater. Design.*, **31**(10), 4748-4754.

Yeh, I.C. (2008), "Modeling slump of concrete with fly ash and superplasticizer", *Comput. Concrete*, **5**(6), 559-572.

Yilmaz, B. and Ediz, N. (2008), "The use of raw and calcined diatomite in cement production", *Cement Concrete Comp.*, **30**(3), 202-211.

Zuhua, Z., Xiao, Y., Huajun, Z. and Yue, C. (2009), "Role of water in the synthesis of calcined kaolin-based geopolymer", *Appl. Clay Sci.*, **43**(2), 218-223.

CC

4. Sinsiri, T.*, Kroehong, W, Jaturapitakkul, C., Chindaprasirt, P., 2012, Assessing the effect of biomass ashes with different finenesses on compressive strength of blended cement paste, Materials and Design, Vol. 42, pp. 424-433. (IF= 2.200)

JMAD 4606
29 June 2012
ARTICLE IN PRESS
No. of Pages 11, Model 5G

Materials and Design xxx (2012) xxx–xxx

Contents lists available at SciVerse ScienceDirect

Materials and Design

journal homepage: www.elsevier.com/locate/matdes

Assessing the effect of biomass ashes with different finenesses on the compressive strength of blended cement paste

Theerawat Sinsiri[a,*], Wunchock Kroehong[a], Chai Jaturapitakkul[b], Prinya Chindaprasirt[c]

[a] School of Civil Engineering, Institute of Engineering, Suranaree University of Technology, Nakorn Ratchasima 30000, Thailand
[b] Department of Civil Engineering, Faculty of Engineering, King Mongkut's University of Technology Thonburi, Bangkok 10140, Thailand
[c] Sustainable Infrastructure Research and Development Center, Department of Civil Engineering, Faculty of Engineering, Khon Kaen University, Khon Kaen 40002, Thailand

ARTICLE INFO

Article history:
Received 28 March 2012
Accepted 16 June 2012
Available online xxxx

Keywords:
Rice husk ash
Palm oil fuel ash
Amorphous
Hydration reaction
Filler effect
Pozzolanic reaction

ABSTRACT

This study assesses the effect of biomass ashes with different finenesses on the compressive strength of blended cement paste. rice husk ash (RHA), palm oil fuel ash (POFA) and river sand (RS) were ground to obtain two finenesses: one was the same size as the cement, and the other was smaller than the cement. Type I Portland cement was replaced by RHA, POFA and RS at 0%, 10%, 20%, 30% and 40% by weight of binder. A water to binder ratio (W/B) of 0.35 was used for all blended cement paste mixes. The percentages of amorphous materials and the compressive strength of the pastes due to the hydration reaction, filler effect and pozzolanic reaction were investigated. The results showed that ground rice husk ash and ground palm oil fuel ash were composed of amorphous silica material. The compressive strength of the pastes due to the hydration reaction decreased with decreasing cement content. The compressive strength of the pastes due to the filler effect increased with increasing cement replacement. The compressive strengths of the pastes due to the pozzolanic reaction were nonlinear and were fit with nonlinear isotherms that increased with increasing fineness of RHA and POFA, cement replacement rate and age of the paste. In addition, the model that was proposed to predict the percentage compressive strength of the blended cement pastes on the basis of the age of the paste and the percentage replacement with biomass ash was in good agreement with the experimental results. The optimum replacement level of rice husk ash and palm oil fuel ash in pastes was 30% by weight of binder; this replacement percentage resulted in good compressive strengths.

1. Introduction

In the manufacture of cement, the clinker production process requires a great amount of energy and emits a large amount of carbon dioxide (CO_2) into the atmosphere. According to the Intergovernmental Panel on Climate Change (IPCC), the production of cement in 2005 accounted for approximately 7% of the CO_2 emissions worldwide [1]. Global cement production will increase by an average of 2.1% every year between 2005 and 2030, reaching a level that is 1.7 times greater than that in 2005 because of the growth of countries [2]. The increase in CO_2 emissions has led to the greenhouse effect and an increase in the earth's temperature. The environmental impact of cement production must be reduced by reducing the production of ordinary Portland cement. To reduce the environmental problems, pozzolanic materials, such as fly ash, silica fume and agro-waste ashes, are used as mineral admixtures to reduce the production of cement, thus reducing the emission of CO_2 and the use of energy. This solution has been reported to be environmentally friendly. In addition, the incorporation of mineral admixtures in concrete can also improve the mechanical properties and durability of the concrete [3–5].

Rice husk ash (RHA) is a by-product of electricity generation biomass power plants. In Thailand, the annual production of RHA has been approximated at 1.6 million tons [6]. Several researchers have shown that the main chemical composition of rice husk is silicon dioxide (SiO_2), and the highest amount of amorphous silica was achieved when rice husk ash was burned between 500 and 700 °C [7,8]. Thus, RHA is a pozzolanic material and can be used as a supplementary cementitious material to replace Type I Portland cement by up to 30% [9,10]. Rukzon et al. [11] found that rice hush ash with high fineness can improve the compressive strength and produce a mortar with low porosity. For durability, the results showed that the use of RHA to partially replace Type I Portland cement improves the concrete water permeability [12], chloride penetration [10,13], and resistance to deterioration due to sulfate [3,4].

Palm oil fuel ash (POFA) is a by-product of palm oil factories, where palm shells, empty fruit bunches and palm fiber are burnt as fuel at temperatures of 800–900 °C. It has been estimated that more than 100,000 tons of palm oil fuel ash are produced in

* Corresponding author. Tel.: +66 4422 4420; fax: +66 4422 4607.
E-mail address: sinsiri@sut.ac.th (T. Sinsiri).

0261-3069/$ - see front matter © 2012 Published by Elsevier Ltd.
http://dx.doi.org/10.1016/j.matdes.2012.06.030

JMAD 4606
29 June 2012
ARTICLE IN PRESS
No. of Pages 11, Model 5G

Thailand every year [14]. Palm oil fuel ash is rarely utilized, and the amount produced is increasing annually. Previous researchers have found that POFA is a pozzolanic material, and ground POFA with high fineness can be used to replace Type I Portland cement at a rate of up to 30% by weight of binder. Chindaprasirt et al. [13] indicated that POFA improves the compressive strength and provides good resistance to chloride penetration. Tangchirapat and Jaturapitakkul [15] showed that POFA with high fineness can reduce the drying shrinkage and water permeability of concrete.

Cyr et al. [16] reported that the effect of mineral admixtures on the compressive strength involved three factors. First, the dilution effect is the strength proportional to the amount of cement in the mixture. Second, the physical effect is the strength that depends on the fineness and the amount of powder, which lead to the nucleation effect and filler effect. The nucleation effect accelerates the hydration production and leads to a more homogeneous paste. The filler effect is due to a suitable arrangement of small particles that fill the voids of the paste and increase its compressive strength. Third, the pozzolanic reaction occurs between $Ca(OH)_2$ and the SiO_2 and Al_2O_3 from pozzolanic materials, which produces an increase in calcium silicate hydrate C–S–H [17–19]. However, many researchers have studied the pozzolanic reaction, using, for example, ASTM C618, strength activity index ASTM C311, X-ray diffraction (XRD), thermogravimetric analysis (TGA) and chemical titration. Moreover, Tangpagasit et al. [20] studied the use of river sand as an inert material to replace Type I Portland cement to evaluate the packing effect and pozzolanic reaction of fly ash in mortar. They found that river sand is an inert material and that the packing effect is not dependent on the age of the mortar but rather on the particle size while the pozzolanic reaction depends on the fineness and age of the mortar.

Previous studies have already reported the influence of the finenesses of RHA and POFA on the compressive strength and observed that ashes with a median particle size larger than OPC (~15 μm) can be used to replace OPC at 10% [10] while smaller sizes than OPC can be used at 20% to 30% by weight of binder [15]. However, the separation of the influences of the hydration reaction, the filler effect and the pozzolanic reaction on compressive strength of blended cement pastes has not been well defined. If a by-product material from biomass plants can be used as a cement replacement in concrete, it will help reduce energy use by reducing the production of cement clinker and reducing the volume of waste disposed to landfills. Thus, the objective of this study is to quantify the effect of the hydration reaction, the filler effect and the pozzolanic reaction on compressive strength of paste. In addition, equation derived from results determine from experimental testing was derived to predict the compressive strength of a paste due to the hydration reaction, filler effect, and pozzolanic reaction. The chemical properties and percentages of amorphous materials were investigated. The effects of ground rice husk ash and ground palm oil fuel ash with two different finenesses, which influences the hydration reaction, filler effect, and pozzolanic reaction, on the compressive strength of blended cement pastes were determined.

2. Experimental details

2.1. Materials

The materials used in this study were Type I Ordinary Portland cement (OPC), rice husk ash (RHA), palm oil fuel ash (POFA), and river sand. RHA and POFA were collected from thermal power plants in Thailand, and the inert material used was ground river sand (RS). The original RHA and POFA had large particles with low pozzolanic properties [11,21]. Thus, the original RHA and POFA were sieved through a sieve No. 16 to remove the large particles and any incompletely combusted material. The difference in compressive strength between the pozzolan paste and inert material paste can be determined as the compressive strength due to the pozzolanic reaction [20]. Then, the RHA, POFA and RS were ground to two different sizes. To eliminate the filler effect, RHA, POFA and RS were ground to have the same particle size as OPC for the first fineness of materials (CRHA, CPOFA and CRS). For the second fineness from the filler effect of materials (FRHA, FPOFA and FRS), the materials were ground to have particles that could act as fillers between the particles of cement by an attrition mill for 60 min at 1000 rpm using 2 mm diameter steel balls.

As shown in Fig. 1a, if the median particle size of a material is the same as that of OPC (~15 μm), the filler should have the save particle size as OPC.

$$d = D = 15\mu m \tag{1}$$

If the median particle size of the material is smaller than that of cement and acts as filler between the particles of cement, as shown in Fig. 1(b), the median size of the material can be calculated with Eq. (3) [22]:

$$d = cos30^{\circ}\frac{D/2}{D/2 + d/2} \tag{2}$$

$$d = 0.15D = 0.15(15) = 2.25\mu m \tag{3}$$

The SEM photographs of the materials are shown in Fig. 2. It was found that the ground RHA and POFA consisted of irregular, crushed particles. A similar conclusion was also reported by other researchers [13]. The physical properties of the materials are presented in Table 1. The first group of materials (CRHA, CPOFA and CRS) had particle sizes equal to that of cement. The specific gravity of CRHA, CPOFA and CRS was 2.29, 2.36 and 2.59, respectively. The Blaine fineness values of CRHA, CPOFA and CRS were 7600, 6700 and 3900 cm^2/g, respectively. For the small particle group (FRHA, FPOFA and FRS), the specific gravity and Blaine fineness of FRHA, FPOFA and FRS were 2.31, 2.48, 2.61 and 18,000, 14,900 and 6300 cm^2/g, respectively. The particle size distributions of the materials are shown in Fig. 3. The median particle sizes of CRHA, CFOFA and CRS were close to the particle size of the cement, while those of FRHA, FPOFA and FRS were smaller than that of cement.

2.2. Mix proportion

Ground RHA, POFA and RS were used to partially replace Type I Portland cement at the rates of 0%, 10%, 20%, 30% and 40% by weight of binder. A water to binder (W/B) ratio of 0.35 was used for all mixtures and is shown in Table 2. To ensure homogeneity, the OPC, RHA, POFA and RS were first mixed together for 3 min in the mixer, and then the water was added. Afterwards, the mixture was mixed for another 2 min. After mixing, the cement pastes were immediately cast into cube specimens of 50 × 50 × 50 mm. The cast specimens were covered with plastic to prevent water loss. After casting for 24 h, the specimens were removed from the molds and cured in saturated lime water at a temperature of 23 ± 2 °C.

2.3. Compressive strength

The cube specimens of 50 × 50 × 50 mm were prepared in accordance with ASTM C109 [23]. They were tested to determine the compressive strength at the ages of 7, 28, 60 and 90 days. Each compressive strength value reported is the average of five samples.

Please cite this article in press as: Sinsiri T et al. Assessing the effect of biomass ashes with different finenesses on the compressive strength of blended cement paste. J Mater Design (2012), http://dx.doi.org/10.1016/j.matdes.2012.06.030

JMAD 4606
29 June 2012
ARTICLE IN PRESS
No. of Pages 11, Model 5G

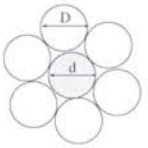

(a) Median particle size equal to that of OPC

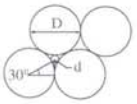

(b) Minimum median particle size

Fig. 1. Plan view illustration of the relationship between the particles of cement.

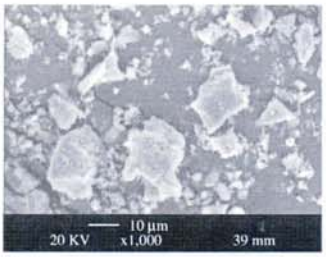

(a) Ground coarse rice husk ash (CRHA)

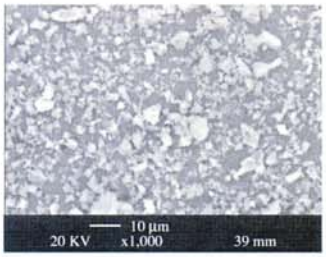

(b) Ground fine rice husk ash (FRHA)

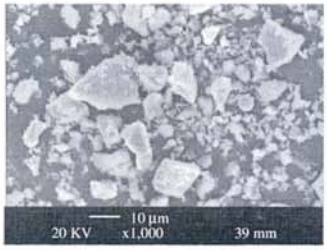

(c) Ground coarse palm oil fuel ash (CPOFA)

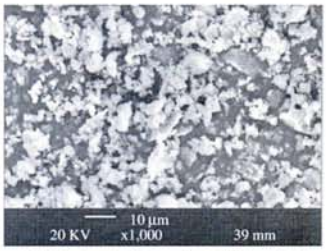

(d) Ground fine palm oil fuel ash (FPOFA)

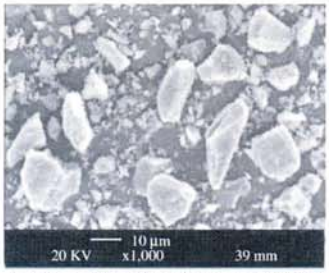

(e) Ground coarse river sand (CRS)

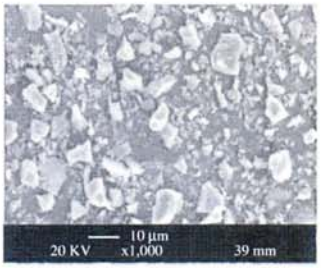

(f) Ground fine river sand (FRS)

Fig. 2. Scanning electron micrographs of the materials.

Table 1
Physical properties of the materials.

Sample (cm^2/g)	Specific gravity	Median particle size, d_{50} (µm)	Blaine fineness
OPC	3.14	14.6	3600
CRHA	2.29	14.8	7600
CPOFA	2.36	15.6	6700
CRS	2.59	15.9	3900
FRHA	2.31	1.9	18,100
FPOFA	2.48	2.1	14,900
FRS	2.61	2.2	6300

2.3.1. Evaluation of the percentage compressive strength of paste due to the hydration reaction

The percentage compressive strength of a paste due to the hydration reaction (P_H) is the ratio between the compressive strength of the paste containing inert material with the same particle size of cement and the compressive strength of the OPC paste. The percentage compressive strength of a paste due to the hydration reaction is calculated by the following equation:

$$P_H = \left(\frac{C_{ic}}{C_{opc}}\right) \times 100 \quad (4)$$

Please cite this article in press as: Sinsiri T et al. Assessing the effect of biomass ashes with different finenesses on the compressive strength of blended cement paste. J Mater Design (2012), http://dx.doi.org/10.1016/j.matdes.2012.06.030

JMAD 4606
29 June 2012
ARTICLE IN PRESS
No. of Pages 11, Model 5G

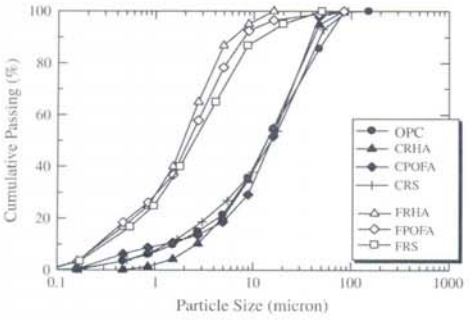

Fig. 3. Particle size distributions of the materials.

where P_H is the percentage compressive strength of the paste due to the hydration reaction (%), C_{ic} is the compressive strength of the paste containing inert material with the same particle size of cement (MPa) and C_{opc} is the compressive strength of OPC paste (MPa).

2.3.2. Evaluation of the percentage compressive strength of paste due to the filler effect

The percentage compressive strength of paste due to the filler effect (P_F) is the difference in the percentage compressive strength between the paste with inert material with high fineness and the paste with inert material with the same particle size as the cement. The percentage compressive strength of paste due to the filler effect is calculated by the following equation:

$$P_F = (P_{lf(p,t)} - P_{ic(p,t)}) \quad (5)$$

where P_F is the percentage compressive strength of the paste due to the filler effect (%), $P_{lf(p,t)}$ is the percentage compressive strength of the paste containing inert material with high fineness compared with OPC paste (%) and $P_{ic,(p,t)}$ is the percentage compressive strength of the paste containing inert material with the same particle size as the cement compared with OPC paste (%). $P_{lf(p,t)}$ and $P_{ic,(p,t)}$ have the same replacement (p) and the same age (t).

2.3.3. Evaluation of the percentage compressive strength due to the pozzolanic reaction

The percentage compressive strength of paste due to the pozzolanic reaction ($P_{PZ,t}$) is the difference in the percentage compressive strength between the RHA or POFA paste and the inert material paste. The percentage compressive strengths of paste due to the pozzolanic reaction were calculated by the following equation:

$$P_{pZ,t} = (P_{b,(p,s,t)} - P_{i(p,s,t)}) \quad (6)$$

where $P_{PZ,t}$ is the percentage compressive strength of the paste due to the pozzolanic reaction (%), $P_{b,(p,s,t)}$ is the percentage compressive strength of the paste containing RHA or POA compared with OPC paste (%) and $P_{i,(p,s,t)}$ is the percentage compressive strength of the paste containing inert material compared with OPC paste (%) $P_{b,(p,s,t)}$ and $P_{i,(p,s,t)}$ have the same replacement (p), fineness (s) and age (t).

3. Results and discussion

3.1. Chemical and mineralogical analysis

The chemical compositions of the materials are shown in Table 3. SiO_2 is the major chemical component of CRHA, FRHA, CPOFA and FPOFA and is 88.8%, 87.8%, 54.0% and 55.7%, respectively. LOI and SO_3 are within the limits of 10.0% and 4%, respectively. The total amounts of SiO_2, Al_2O_3 and Fe_2O_3 in CRHA and FRHA were 91.1% and 89.2%, respectively, which are higher than the 70% for Class N pozzolan specified by ASTM C 618 [24]. However, the total amounts of SiO_2, Al_2O_3 and Fe_2O_3 of CPOFA and FPOFA were 56.9% and 58.6%, respectively, both of which are less than 70%. A similar finding was also reported by other researchers [25]. They found that POFA had a total SiO_2, Al_2O_3 and Fe_2O_3 content less than 70%. In the case of insoluble material (river sand (RS)), the main chemical component of CRS and FRS was also SiO_2 and was 92.0% and 91.2%, respectively. In addition, the X-ray diffraction patterns of the materials are shown in Fig. 4. The percentage of amorphous material was determined by the quantitative XRD analysis based

Table 2
Mixture proportions of the pastes.

Mix No	Symbol	OPC	CRS	CRHA	CPOFA	FRS	FRHA	FPOFA	W/B
1	OPC	100	–	–	–	–	–	–	0.35
2	10CRS	90	10	–	–	–	–	–	0.35
3	20CRS	80	20	–	–	–	–	–	0.35
4	30CRS	70	30	–	–	–	–	–	0.35
5	40CRS	60	40	–	–	–	–	–	0.35
6	10CRHA	90	–	10	–	–	–	–	0.35
7	20CRHA	80	–	20	–	–	–	–	0.35
8	30CRHA	70	–	30	–	–	–	–	0.35
9	40CRHA	60	–	40	–	–	–	–	0.35
10	10CPOFA	90	–	–	10	–	–	–	0.35
11	20CPOFA	80	–	–	20	–	–	–	0.35
12	30CPOFA	70	–	–	30	–	–	–	0.35
13	40CPOFA	60	–	–	40	–	–	–	0.35
14	10FRS	90	–	–	–	10	–	–	0.35
15	20FRS	80	–	–	–	20	–	–	0.35
16	30FRS	70	–	–	–	30	–	–	0.35
17	40FRS	60	–	–	–	40	–	–	0.35
18	10FRHA	90	–	–	–	–	10	–	0.35
19	20FRHA	80	–	–	–	–	20	–	0.35
20	30FRHA	70	–	–	–	–	30	–	0.35
21	40FRHA	60	–	–	–	–	40	–	0.35
22	10FPOFA	90	–	–	–	–	–	10	0.35
23	20FPOFA	80	–	–	–	–	–	20	0.35
24	30FPOFA	70	–	–	–	–	–	30	0.35
25	40FPOFA	60	–	–	–	–	–	40	0.35

Please cite this article in press as: Sinsiri T et al. Assessing the effect of biomass ashes with different finenesses on the compressive strength of blended cement paste. J Mater Design (2012), http://dx.doi.org/10.1016/j.matdes.2012.06.030

JMAD 4606
29 June 2012
ARTICLE IN PRESS
No. of Pages 11, Model 5G

Table 3
Chemical compositions of the materials.

Chemical composition (%)	OPC	CRHA	FRHA	CPOFA	FPOFA	CRS	FRS
Silicon dioxide (SiO_2)	20.8	88.8	87.8	54.0	55.7	92.0	91.2
Aluminum oxide (Al_2O_3)	4.7	0.6	0.5	0.9	0.9	1.6	1.8
Iron oxide (Fe_2O_3)	3.4	1.7	0.9	2.0	2.0	0.6	0.2
Calcium oxide (CaO)	65.3	1.1	1.2	12.9	12.5	0.9	0.7
Magnesium oxide (MgO)	–	0.6	0.6	4.9	5.1	0.1	0.1
Sodium oxide (Na_2O)	0.1	0.2	0.2	1.0	1.0	0.1	0.1
Potassium oxide (K_2O)	0.4	2.0	2.2	13.5	11.9	2.2	2.3
Sulfur trioxide (SO_3)	2.7	0.1	0.1	4.0	2.9	–	–
Loss on ignition (LOI)	0.9	3.6	5.2	3.7	4.7	2.1	1.8
$SiO_2 + Al_2O_3 + Fe_2O_3$	–	91.1	89.2	56.9	58.6	94.2	93.2
Quantitative XRD, Rietveld method							
Amorphous (%)	–	70.1	69.6	70.2	67.2	–	–
Crystalline (%)	–	29.9	30.4	29.8	32.8	100.0	100.0
Quartz	–	59.3	56.2	65.0	73.0	100.0	100.0
Cristobalite	–	40.7	43.8	35.0	27.0	–	–

on the Rietveld method, which was calculated using Bruker's TOPAS. The amorphous contents of CRHA, FRHA, CPOFA and FPOFA were 70.1%, 69.6%, 70.2% and 67.2% (by mass), respectively. The percentages of crystalline CRS and FRS were 100% (by mass). The results confirm that river sand is an inert material, which is similar to the results of previous research [20].

3.2. Compressive strength

Table 4 shows the compressive strengths at 7, 28, 60 and 90 days for the OPC paste, which were 53.0, 75.0, 84.6 and 99.1 MPa, respectively. At 7 days, the compressive strengths of pastes containing 10–40% of CRHA with the same particle size as cement were lower than that of the OPC paste because of the low cement content, which resulted in a significant reduction in the normalized strength [15,26]. Additionally, the compressive strengths of the 10CRHA and 20CRHA pastes at 28 days were 76.5 and 74.2 MPa or about 102% and 98.9% of that of the OPC paste, respectively, while those of the 30CRHA and 40CRHA pastes at 28 and 90 days were 70.5, 64.7 and 100.0, 92.1 MPa or about 94%, 86.3% and 100.9%, 92.9% of that of the OPC paste, respectively. In the case of pastes containing FRHA (small particle size of RHA), the compressive strengths of the 10FRHA, 20FRHA and 30FRHA pastes were 55.9, 52.9 and 50.3 MPa or 105.5%, 99.8% and 94.9% of that of the OPC paste at 7 days but increased to 81.7, 78.7 and 74.9 MPa or 108.9%, 104.9% and 99.9% of that of the OPC paste at 28 days, respectively.

For the group mixed with ground palm oil fuel ash, the pastes containing 10–40% CPOFA had compressive strengths that were lower than that of OPC paste at 7 days. The 28 days compressive strengths were 74.8, 72.0, 66.7 and 61.5 MPa with a normalized strength of 99.7%, 96.0%, 88.9% and 82.0% for the 10CPOFA, 20CPOFA, 30CPOFA and 40CPOFA pastes, respectively. At 90 days, they increased to 104.5, 102.0, 97.1 and 88.1 MPa with a normalized strength of 105.4%, 102.9%, 98.0% and 88.9% of the OPC paste, respectively. For the pastes with a small particle size, the compressive strengths of the 10FPOFA and 20FPOFA pastes at 28 and 90 days were 79.3, 77.3 and 111.3, 109.6 MPa or about 105.7%, 103.1% and 112.3%, 110.6% of the strength of the OPC paste, respectively. However, at 30% and 40% FPOFA, the compressive strengths at 90 days were 104.0 and 94.1 MPa or about 104.9% and 95.0% of that of the OPC paste, respectively.

The compressive strength of blended cement paste increased with age but decreased with an increase in the replacement of ash. The increased compressive strength of blended cement paste can be explained by three factors: the hydration reaction, the filler effect and the pozzolanic reaction. The hydration reaction is the strength proportionate to the amount of cement in the mix. The filler effect has two causes, the nucleation effect and packing effect, which depend significantly on the fineness of material. The nucleation effect arises when the small particles are dispersed in the blended cement paste and enhance the cement hydrate while the packing effect occurs when small particles fill the voids of the paste [16,18,27,28]. Therefore, the blended cement paste containing biomass ash with high fineness was more homogeneous and denser, which increased the compressive strength of the paste. Finally, the pozzolanic reaction occurs because of the SiO_2 and Al_2O_3 contained in the biomass ash, which react with $Ca(OH)_2$ and produce an additional calcium silicate hydrate (C–S–H).

Comparing the RHA and POFA blended cement pastes in terms of the same replacement and same fineness, the normalized strengths of RHA pastes were slightly higher than those of POFA pastes because RHA contains more SiO_2 than POFA. The results indicated that RHA was more reactive than POFA, and the results agree with [20]. In addition, the results suggest that the replacement of cement type I by RHA and POFA up to 30% by weight of binder does not impair the compressive strength of pastes. The results are nearly identical to the results obtained by other researchers [10,29], who reported that the optimum replacement level of Portland cement Type I by RHA or POFA is 30% by weight of binder.

3.3. Influence of cement content on the percentage compressive strength of paste

The percentage compressive strength of ground river sand paste with age (P_H) is shown in Fig. 5. For pastes containing CRS with the same particle size as that of cement, the percentage compressive strengths of CRS pastes at any age were almost constant. The same trend was also reported by [20,29]. In contrast, the relationship between the percentage compressive strengths of pastes due to the hydration reaction and the percentage replacement of CRS paste is shown in Fig. 6. The percentage compressive strengths decreased linearly with replacement of CRS. The results suggest that the percentage compressive strength of pastes containing inert material with the same particle size as cement does not depend on age but rather depends on the cement content.

The empirical equations can be expressed for the percentage compressive strength of paste due to the hydration reaction in terms of (R) as follows:

$$P_H = 100.4 - 0.996(R) \quad (7)$$

where P_H is percentage compressive strength due to the hydration reaction of paste (%) and R is the replacement of Portland cement by an inert material (%). The correlation value of 0.997 indicates a

Please cite this article in press as: Sinsiri T et al. Assessing the effect of biomass ashes with different finenesses on the compressive strength of blended cement paste. J Mater Design (2012), http://dx.doi.org/10.1016/j.matdes.2012.06.030

JMAD 4606
29 June 2012
ARTICLE IN PRESS
No. of Pages 11, Model 5G

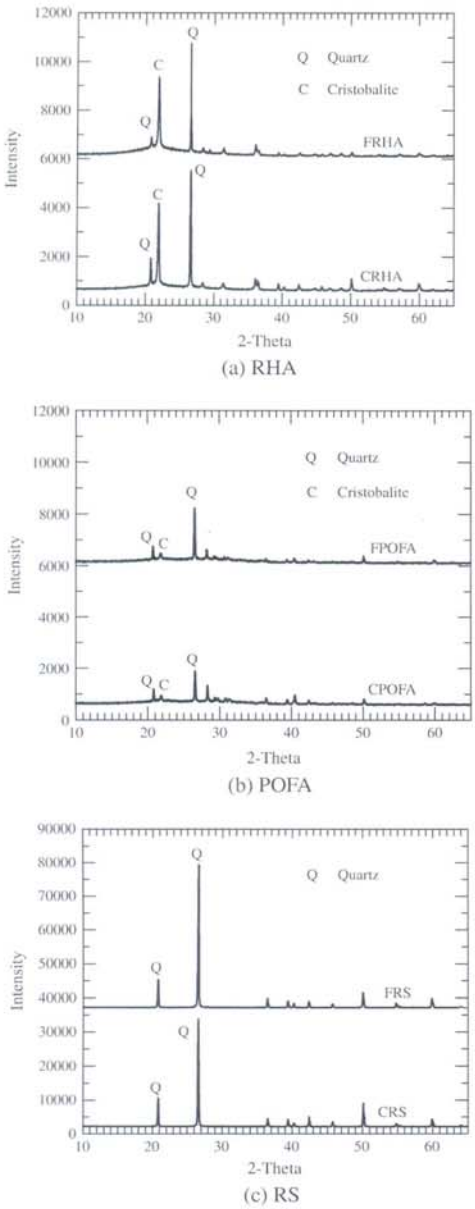

Fig. 4. X-ray diffraction patterns of the materials.

strong linear relationship between the percentage compressive strength and the percentage replacement of CRS.

3.4. Influence of the filler effect on the percentage compressive strength of paste

The relationship between the percentage compressive strength of ground river sand with different finenesses of paste and age are shown in Fig. 5. The pastes with particles smaller than OPC had a higher percentage compressive strength than the pastes with large particle size and had an almost constant value [20,29]. Fig. 7 shows the percentage compressive strengths of ground river sand with different finenesses of paste and replacements with river sand. The percentage compressive strength of paste due to the filler effect tended to increase with the amount of cement replacement and was approximately 2.2–5.1% of the strength of the OPC paste because the small particles dispersed into the blended cement paste and accelerated the hydration reaction. In addition, the packing effect occurred as the small particles filled the voids of the paste [16,18,27,28]. Therefore, the paste was more homogeneous and denser, which resulted in the increased compressive strength of the paste. These results suggest that a particle size smaller than OPC has very important role in increasing the compressive strength because of the filler effect [30]. The results of the filler effect for pastes agrees closely with the result obtained by Jaturapitakkul et al. [31], who reported that the difference in the percentage compressive strengths between mortar containing the same particle sizes of inert material and small sizes of inert material was up to 5.8% of the strength of the mortar.

The empirical equation to predict the percentage of the compressive strength of the paste due to the filler effect in terms of replacement (R) is proposed as follows:

$$P_F = 1.542Ln(R) - 1.002 \quad (8)$$

where P_F is the percentage compressive strength of the paste due to the filler effect (%) and R is the replacement of Portland cement by inert material (%). It was found that P_F is represented by a logarithmic equation and has good correlation. The percentage compressive strength of the paste due to the filler effect of the blended cement paste increased with an increase in the replacement of inert material.

3.5. Influence of the pozzolanic reaction on the percentage compressive strength of pastes

Figs. 8 and 9 show the percentage compressive strength of paste due to the pozzolanic reaction of RHA and POFA, respectively. The pozzolanic reaction increased with age and with the replacement of RHA or POFA. In addition, the high fineness of RHA or POFA was more efficient for the pozzolanic reaction than the coarse fineness because the high fineness of the ash provided a large surface area to contribute silica and alumina compounds for the pozzolanic reaction [32,33]. These compounds reacted with $Ca(OH)_2$ from the hydrated cement and produced an increase in calcium silicate hydrate. In addition, the percentage compressive strength due to the pozzolanic reaction of higher replacement paste increased more than that of the lower replacement paste. The blended cement paste containing a high replacement of the ash showed a decrease of $Ca(OH)_2$ content compared with the low replacement paste [34]. In addition, the reduction of $Ca(OH)_2$ affected the increase of the calcium silicate hydrate from the pozzolanic reaction [35].

Comparing the percentage compressive strength of paste due to the pozzolanic reaction in Figs. 8 and 9, the RHA pastes had a higher percentage compressive strength of paste due to the pozzolanic reaction than the POFA pastes. The maximum percentage compressive strength due to the pozzolanic reaction of RHA and POFA pastes were 33.7% and 30.5% that of the OPC paste, respectively, because RHA has a higher SiO_2 content than POFA. The results confirmed that the percentage compressive strength of paste due to the pozzolanic reaction increased with age, fineness, and the replacement rate of the ash.

Figs. 8 and 9 show that the percentage compressive strength due to the pozzolanic reaction is explicitly nonlinear and is best fit with nonlinear isotherms, which are shown in the same figure.

Please cite this article in press as: Sinsiri T et al. Assessing the effect of biomass ashes with different finenesses on the compressive strength of blended cement paste. J Mater Design (2012), http://dx.doi.org/10.1016/j.matdes.2012.06.030

JMAD 4606
29 June 2012
ARTICLE IN PRESS
No. of Pages 11, Model 5G

Table 4
Compressive strengths of the pastes.

Symbol	Compressive strength (MPa)				Normalized compressive strength (%)			
	7 days	28 days	60 days	90 days	7 days	28 days	60 days	90 days
OPC	53.0	75.0	84.6	99.1	100.0	100.0	100.0	100.0
10CRHA	52.4	76.5	88.5	107.6	98.9	102.0	104.6	108.6
20CRHA	49.8	74.2	88.3	106.0	94.0	98.9	104.4	107.0
30CRHA	46.5	70.5	83.7	100.0	87.7	94.0	98.9	100.9
40CRHA	42.4	64.7	77.4	92.1	80.0	86.3	91.5	92.9
10FRHA	55.9	81.7	94.7	116.2	105.5	108.9	111.9	117.3
20FRHA	52.9	78.7	93.1	113.2	99.8	104.9	110.0	114.2
30FRHA	50.3	74.9	89.6	107.9	94.9	99.9	105.9	108.9
40FRHA	44.5	66.9	79.5	96.1	84.0	89.2	94.0	97.0
10CPOFA	51.3	74.8	86.3	104.5	96.8	99.7	101.6	105.4
20CPOFA	48.3	72.0	84.6	102.0	91.1	96.0	99.6	102.9
30CPOFA	44.5	66.7	78.6	97.1	84.0	88.9	92.9	98.0
40CPOFA	41.0	61.5	72.8	88.1	77.4	82.0	85.7	88.9
10FPOFA	53.7	79.3	93.3	111.3	101.3	105.7	109.9	112.3
20FPOFA	51.9	77.3	92.2	109.6	97.9	103.1	108.6	110.6
30FPOFA	48.3	72.8	86.3	104.0	91.1	96.9	101.6	104.9
40FPOFA	44.0	66.5	78.6	94.1	83.0	88.7	92.6	95.0
10CRS	48.3	68.2	77.2	90.1	91.1	90.9	91.3	90.9
20CRS	42.9	60.8	67.9	78.6	80.9	81.1	80.3	79.3
30CRS	36.9	53.1	60.8	70.2	69.6	70.8	71.9	70.8
40CRS	31.5	45.6	51.5	59.6	59.4	60.8	60.9	60.1
10FRS	49.9	69.9	79.1	92.8	94.2	93.2	93.5	93.6
20FRS	45.0	63.4	70.8	82.1	84.9	84.5	83.7	82.8
30FRS	39.1	56.5	64.1	74.5	73.8	75.3	75.8	75.2
40FRS	34.2	49.2	55.4	63.9	64.5	65.6	65.5	64.5

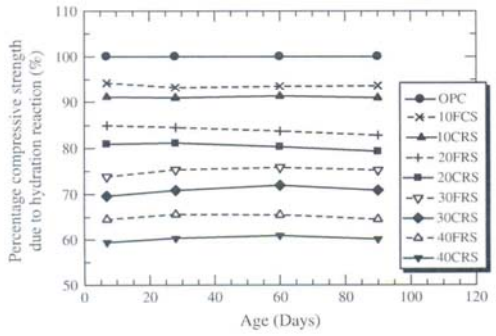

Fig. 5. Relationship between the percentage compressive strength of ground river sand paste and age.

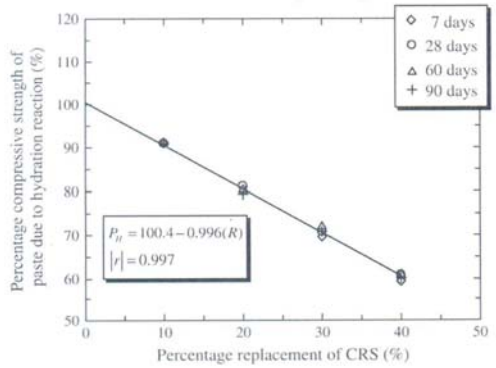

Fig. 6. Relationship between the percentage compressive strength of paste due to the hydration reaction and the percentage replacement of CRS.

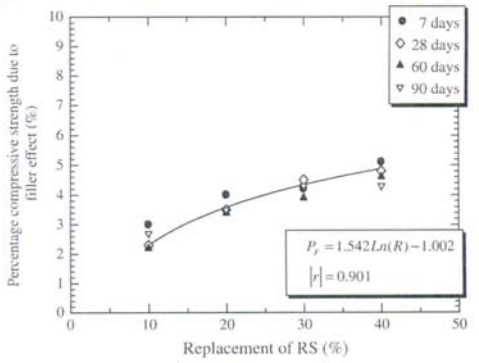

Fig. 7. Relationships between the percentage compressive strength of paste due to the filler effect and the replacement of RS.

Thus, the equation to predict the percentage compressive strength of paste due to the pozzolanic reaction is:

$$P_{PZ,t} = \alpha R^{\beta} \quad (9)$$

where $P_{PZ,t}$ is the percentage compressive strength of the paste due to the pozzolanic reaction at a specified age (t = 7, 28, 60 and 90 days) (%), R is the rice husk ash or palm oil fuel ash replacement (%) and α and β are the pozzolanic constants. The pozzolanic constants for the isotherm fitted from experimental results of the pastes are presented in Table 5.

3.6. Generating an empirical equation for the prediction of the percentage compressive strength of the blended cement paste

3.6.1. Role of the blended cement paste containing biomass ash on the percentage of compressive strength

The percentage compressive strength of the blended cement paste containing biomass ash with the same particle size as cement

Please cite this article in press as: Sinsiri T et al. Assessing the effect of biomass ashes with different finenesses on the compressive strength of blended cement paste. J Mater Design (2012), http://dx.doi.org/10.1016/j.matdes.2012.06.030

JMAD 4606
29 June 2012
ARTICLE IN PRESS
No. of Pages 11, Model 5G

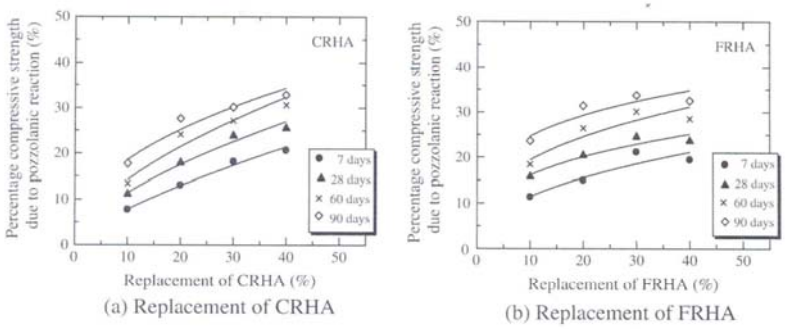

Fig. 8. Relationships between the percentage compressive strength due to the pozzolanic reaction of RHA pastes and age.

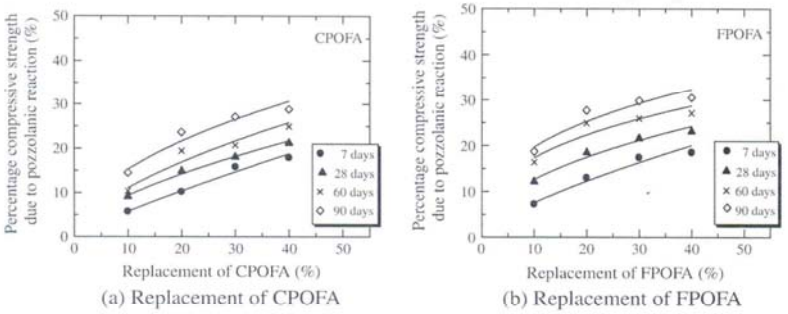

Fig. 9. Relationships between the percentage compressive strength due to the pozzolanic reaction of POFA paste and age.

Table 5
Best fit of the pozzolanic constants for the isotherms.

Binder Type	Days	Pozzolanic constants		Correlation
		α	β	
CRHA	7	1.479	0.723	0.993
	28	2.728	0.617	0.988
	60	3.593	0.595	0.948
	90	6.633	0.445	0.943
FRHA	7	4.098	0.444	0.895
	28	7.667	0.321	0.923
	60	8.817	0.341	0.865
	90	13.940	0.247	0.837
CPOFA	7	0.792	0.856	0.993
	28	2.273	0.611	0.991
	60	2.703	0.611	0.939
	90	4.798	0.502	0.949
FPOFA	7	1.462	0.709	0.972
	28	4.590	0.449	0.974
	60	7.513	0.363	0.884
	90	8.551	0.361	0.899

is related to the hydration reaction and pozzolanic reaction as follows:

$$P_{C,t} = P_H + P_{PZ,t} \tag{10}$$

Eq. (10) can be rewritten as follows:

$$P_{C,t} = 100.4 - 0.99(R) + \alpha R^{\beta} \tag{11}$$

where $P_{C,t}$ is the total percentage compressive strength of the paste at a specified age (t = 7, 28, 60 and 90 days) (%), P_H is the percentage compressive strength of the paste due to the hydration reaction (%), $P_{PZ,t}$ is the percentage compressive strength of the paste due to the pozzolanic reaction at various curing times (t = 7, 28, 60 and 90 days) (%), R is the percentage replacement of RHA or POFA and α and β are the pozzolanic constants. The prediction using Eq. (11) and experimental results are shown in Fig. 10. This equation is useful to predict the percentage compressive strength of blended cement pastes containing RHA and POFA.

For the mixture of biomass ash with a particle size smaller than that of OPC, the percentage compressive strength of paste is due to the hydration reaction, filler effect and pozzolanic reaction as follows:

$$P_{C,t} = P_H + P_F + P_{PZ,t} \tag{12}$$

Eq. (12) can be rewritten as follows:

$$P_{C,t} = 99.398 - 0.996(R) + 1.542Ln(R) + \alpha R^{\beta} \tag{13}$$

where $P_{C,t}$ is the total percentage compressive strength of the paste at a specified age (t = 7, 28, 60 and 90 days) (%), P_H is the percentage compressive strength of the paste due to the hydration reaction (%), P_F is the percentage compressive strength of the paste due to the filler effect (%), $P_{PZ,t}$ is the percentage compressive strength of the paste due to the pozzolanic reaction at a specified age (t = 7, 28, 60 and 90 days) (%), R is the percentage replacement of RHA or POFA, and α and β are the pozzolanic constants. The percentage compressive strength of the pastes according to this equation was compared with the actual test specimens, as shown in Fig. 11. The equation suggests that the percentage compressive strength of the paste due to the pozzolanic reaction is higher than that due to the filler effect. Moreover, it is also useful to predict the percentage

Please cite this article in press as: Sinsiri T et al. Assessing the effect of biomass ashes with different finenesses on the compressive strength of blended cement paste. J Mater Design (2012), http://dx.doi.org/10.1016/j.matdes.2012.06.030

JMAD 4606
29 June 2012
ARTICLE IN PRESS
No. of Pages 11, Model 5G

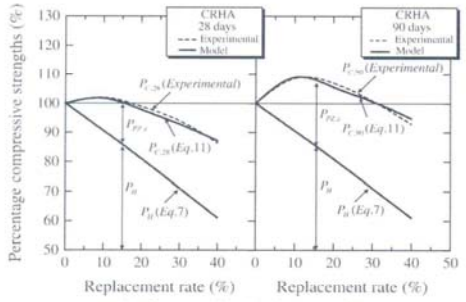

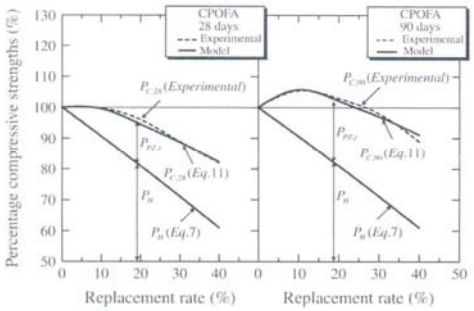

Fig. 10. Relationships between the percentage compressive strengths of blended cement pastes containing CRHA and CPOFA with the same particle size as that of OPC.

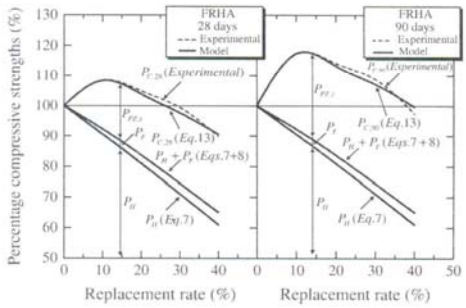

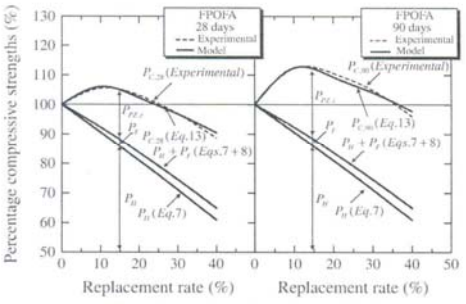

Fig. 11. Relationships between the percentage compressive strengths of the blended cement paste containing FRHA and FPOFA with particle sizes smaller than that of OPC.

compressive strength of pastes with the curing time and amounts of replacement of RHA and POFA.

3.6.2. Verification

The measured percentage compressive strengths of the pastes for $W/B = 0.35$, $R = 10–40\%$, and $d = 7, 28, 60$ and 90 days were compared with the predicted results according to Eqs. (11) and (13), which are shown in Fig. 12. The measured and predicted values are reasonably close. The error from prediction is satisfied with the mean absolute percent error, $\left(\Sigma\left|\frac{P_{predict}-P_{test}}{P_{test}}\right| \times 100\%\right)$, which is less than 2.4%.

4. Conclusions

The results of this study provide the following conclusions.

1. The percentage compressive strength of the pastes due to the hydration reaction decreased with decreasing cement content. In addition, the percentage compressive strength of the paste due to the hydration reaction showed a linear best-fit relationship.
2. Ground inert material with particle sizes smaller than that of OPC was a very important factor affecting the percentage compressive strength due to the filler effect. In addition, the percentage compressive strength of pastes due to the filler effect increased with increasing inert matter material replacement. The percentage compressive strength of pastes due to the filler effect can be predicted with a logarithmic best-fit relationship.

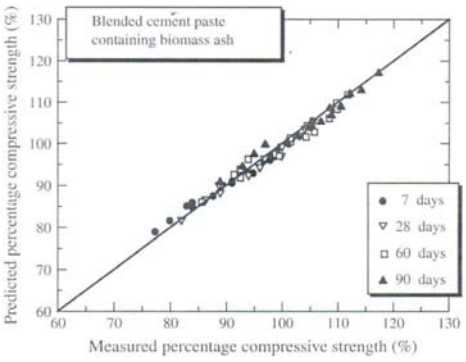

Fig. 12. Comparison between the predicted and experimental percentage compressive strength in blended cement pastes containing biomass ash.

3. The percentage compressive strength of paste due to the pozzolanic reaction increased with increasing fineness of RHA or POFA, cement replacement and age of paste. Moreover, it had a greater effect than the filler effect. The percentage compressive strength due to the pozzolanic reaction is explicitly nonlinear.
4. The use of RHA or POFA with particle sizes smaller than those of OPC to replace Portland cement Type I at the rate of 30% by weight of binder resulted in good compressive strength from filler effect and pozzlanic reaction. Moreover, the proposed

Please cite this article in press as: Sinsiri T et al. Assessing the effect of biomass ashes with different finenesses on the compressive strength of blended cement paste. J Mater Design (2012), http://dx.doi.org/10.1016/j.matdes.2012.06.030

JMAD 4606
29 June 2012
ARTICLE IN PRESS
No. of Pages 11, Model 5G

empirical model can be used to predict the percentage compressive strength of blended cement pastes in good agreement with the experimental results.

Acknowledgments

The authors would like to acknowledge the financial support of the Commission on Higher Education of Thailand for a grant under the Strategic Scholarships for Frontier Research Network for the Joint Ph.D. Program, Thai Doctoral degree. They also thank the Thailand Research Fund (TRF) for the financial support under the TRF Senior Research Scholar, Grant No. RTA5380002 and the TRF New Researcher Scholar, Grant No. MRG5280178.

References

[1] Metz B, Davidson OR, Bosch PR, Dave R, Meyer LA. Climate change 2007. Contribution of working group III to the fourth assessment report of the intergovernmental panel on climate change. Cambridge, United Kingdom and New York, NY, USA: University Press; 2007.
[2] Akashi O, Hanaoka T, Matsuoka Y, Kainuma M. A projection for global CO_2 emissions from the industrial sector through 2030 based on activity level and technology changes. Energy 2011;36(4):1855–67.
[3] Chatveera B, Lertwattanaruk P. Durability of conventional concretes containing black rice husk ash. J Environ Manage 2011;92(1). 59-6.
[4] Chindaprasirt P, Homwuttiwong S, Sirivivatnanon V. Influence of fly ash fineness on strength, drying shrinkage and sulfate resistance of blended cement mortar. Cem Concr Res 2004;34(7):1087–92.
[5] Rukzon S, Chindaprasirt P. Utilization of bagasse ash in high-strength concrete. Mater Des 2012;34:45–50.
[6] Wansom S, Janjaturaphan S, Sinthupinyo S. Characterizing pozzolanic activity of rice husk ash by impedance spectroscopy. Cem Concr Res 2010;40(12):1714–22.
[7] de Sensale GR, Ribeiro AB, Gonçalves A. Effects of RHA on autogenous shrinkage of Portland cement pastes. Cem Concr Compos 2008;30(10):892–7.
[8] Nair DG, Fraaij A, Klaassen AAK, Kentgens APM. A structural investigation relating to the pozzolanic activity of rice husk ashes. Cem Concr Res 2008;38(6):861–9.
[9] Chatveera B, Lertwattanaruk P. Evaluation of sulfate resistance of cement mortars containing black rice husk ash. J Environ Manage 2009;90(3):1435–41.
[10] Ganesan K, Rajagopal K, Thangavel K. Rice husk ash blended cement: assessment of optimal level of replacement for strength and permeability properties of concrete. Constr Build Mater 2008;22(8):1675–83.
[11] Rukzon S, Chindaprasirt P, Mahachai R. Effect of grinding on chemical and physical properties of rice husk ash. Int J Miner Met Mater 2009;16(2):242–7.
[12] Givi AN, Rashid SA, Aziz FNA, Salleh MAM. Assessment of the effects of rice husk ash particle size on strength, water permeability and workability of binary blended concrete. Constr Build Mater 2010;24(11):2145–50.
[13] Chindaprasirt P, Rukzon S, Sirivivatnanon V. Resistance to chloride penetration of blended Portland cement mortar containing palm oil fuel ash, rice husk ash and fly ash. Constr Build Mater 2008;22(5):932–8.
[14] Chindaprasirt P, Homwuttiwong S, Jaturapitakkul C. Strength and water permeability of concrete containing palm oil fuel ash and rice husk-bark ash. Constr Build Mater 2007;21(7):1492–9.
[15] Tangchirapat W, Jaturapitakkul C. Strength, drying shrinkage, and water permeability of concrete incorporating ground palm oil fuel ash. Cem Concr Compos 2010;32(10):767–74.
[16] Cyr M, Lawrence P, Ringot E. Efficiency of mineral admixtures in mortars: quantification of the physical and chemical effects of fine admixtures in relation with compressive strength. Cem Concr Res 2006;36(2):264–77.
[17] Goldman A, Bentur A. The influence of microfillers on enhancement of concrete strength. Cem Concr Res 1993;23(4):962–72.
[18] Gopalan MK. Nucleation and pozzolanic factors in strength development of class F fly ash concrete. ACI Mater J 1993;90(2):117–21.
[19] Isaia GC, Gastaldini ALG, Moraes R. Physical and pozzolanic action of mineral additions on the mechanical strength of high-performance concrete. Cem Concr Compos 2003;25(1):69–76.
[20] Tangpagasit J, Cheerarot R, Jaturapitakkul C, Kiattikomol K. Packing effect and pozzolanic reaction of fly ash in mortar. Cem Concr Res 2005;35(6):1145–51.
[21] Sata V, Jaturapitakkul C, Kiattikomol K. Utilization of palm oil fuel ash in high-strength concrete. J ASCE Mater Civil Eng 2004;16(6):623–8.
[22] Lu N, Likos WJ. Unsaturated soil mechanics. New Jersey: John Wiley & Sons Inc.; 2004.
[23] ASTM C109. Standard test method for compressive strength of hydraulic cement mortars (using 2-in. or [50 mm] cube specimens). Annual book of ASTM standards; 2001.
[24] ASTM C618. Standard specification for coal fly ash and raw or calcined natural pozzolan for use as a mineral admixture in concrete. Annual book of ASTM standards; 2001.
[25] Awal ASMA, Hussin MW. The effectiveness of palm oil fuel ash in preventing expansion due to alkali-silica reaction. Cem Concr Compos 1997;19(4):367–72.
[26] Megat Johari MA, Brooks JJ, Kabir S, Rivard P. Influence of supplementary cementitious materials on engineering properties of high strength concrete. Constr Build Mater 2011;25(5):2639–48.
[27] Montgomery DG, Hughes DC, Williams RIT. Fly ash in concrete – a microstructure study. Cem Concr Res 1981;11(4). 591-03.
[28] Lee C-L, Huang R, Lin W-T, Weng T-L. Establishment of the durability indices for cement-based composite containing supplementary cementitious materials. Mater Des 2012;37:28–39.
[29] Jaturapitakkul C, Tangpagasit J, Songmue S, Kiattikomol K. Filler effect and pozzolanic reaction of ground palm oil fuel ash. Const Build Mater 2011;25(11):4287–93.
[30] Chindaprasirt P, Jaturapitakkul C, Sinsiri T. Effect of fly ash fineness on compressive strength and pore size of blended cement paste. Cem Concr Compos 2005;27(4):425–8.
[31] Jaturapitakkul C, Tangpagasit J, Songmue S, Kiattikomol K. Filler effect of fine particle sand on the compressive strength of mortar. Int J Miner Metal Mater 2011;18(2):240–6.
[32] Cordeiro GC, Toledo Filho RD, Tavares LM, Fairbairn EMR. Pozzolanic activity and filler effect of sugar cane bagasse ash in Portland cement and lime mortars. Cem Concr Compos 2008;30(5):410–8.
[33] Cordeiro GC, Toledo Filho RD, Tavares LM, Fairbairn GC, Hempel S. Influence of particle size and specific surface area on the pozzolanic activity of residual rice husk ash. Cem Concr Compos 2011;33(5):529–34.
[34] Kroehong W, Sinsiri T, Jaturapitakkul C, Chindaprasirt P. Effect of palm oil fuel ash fineness on the microstructure of blended cement paste. Constr Build Mater 2011;25(11). 4095-04.
[35] Aly M, Hashmi MSJ, Olabi AG, Messeiry M, Abadir EF, Hussain AI. Effect of colloidal nano-silica on the mechanical and physical behaviour of waste-glass cement mortar. Mater Des 2012;33:127–35.

Please cite this article in press as: Sinsiri T et al. Assessing the effect of biomass ashes with different finenesses on the compressive strength of blended cement paste. J Mater Design (2012), http://dx.doi.org/10.1016/j.matdes.2012.06.030